IS-T-425





# AN X-RAY DIFFRACTION STUDY OF THE YTTRIA-HAFNIA SYSTEM

Ph. D. Thesis Submitted to Iowa State University, May 1971

Denzil Wayne Stacy

Ames Laboratory, USAEC
Iowa State University
Ames, Iowa 50010

Date Transmitted: June 1971

PREPARED FOR THE U. S. ATOMIC ENERGY COMMISSION
DIVISION OF RESEARCH UNDER CONTRACT NO. W-7405-eng-82

## DISCLAIMER

Available from: National Technical Information Service
Department A
Springfield, VA 22151

Price: Microfiche $0.95

# An X-ray diffraction study of the yttria-hafnia system

by

Denzil Wayne Stacy

A Dissertation Submitted to the
Graduate Faculty in Partial Fulfillment of
The Requirements for the Degree of
DOCTOR OF PHILOSOPHY

Major Subject: Ceramic Engineering

Approved:

D P Wilder
In Charge of Major Work

D P Wilder
Head of Major Department

Dean of Graduate College

Iowa State University
Of Science and Technology
Ames, Iowa

May 1971

# TABLE OF CONTENTS

An X-ray diffraction study of the yttria-hafnia system

Denzil Wayne Stacy

## ABSTRACT

Phase equilibria in the yttria-hafnia system were investigated by high temperature X-ray diffraction and by room temperature X-ray diffraction after fixed temperature anneals. The monoclinic-to-tetragonal phase transformation in hafnia was found to occur over the temperature interval 1750° to 1850°C on heating. The reverse reaction occurred from 1800° to 1550°C on cooling. At 1750°C, the tetragonal unit cell was found to be 2.7 % smaller than the monoclinic unit cell.

Under 2000°C, the solubility of yttria in hafnia is below 1 mole %. The fluorite domain extends from 7 to 53 mole % yttria at 1600°C and from 5 to 55 mole % yttria at 2000°C. A single phase domain of yttria solid solution exists above 73 mole % yttria at 1600° and 2000°C. The fluorite and yttria solid solution domains are separated by a two phase domain.

The liquidus curve remains nearly at the melting point of hafnia (2825°C) up to 40 mole % yttria. Beyond, the liquidus decreases to a minimum of 2340°C at 85 mole % yttria and then increases to the melting point of yttria (2410°C). A tentative phase diagram of the yttria-hafnia system was proposed.

The thermal expansion of yttria and several fluorite compositions was measured by high temperature X-ray diffraction. The mean thermal expansion coefficients of the fluorite compositions from 25° to 2000°C were found to be about $1.1 \times 10^{-5}$ in./in.°C. The mean thermal expansion coefficient for yttria over the same temperature interval was found to be $9.3 \times 10^{-6}$ in./in.°C.

# INTRODUCTION

Hafnia is a most promising refractory material for future nuclear applications. With a very high melting point, extreme chemical inertness, and high thermal neutron capture cross section, its potential uses are as control rods or neutron shielding.

Hafnium occurs in nature with chemically similar zirconium as mixed oxides or silicates. Unlike hafnia, zirconia exhibits a low thermal neutron capture cross section making it useful as cladding for nuclear fuels. This difference in nuclear properties has provided much of the impetus for improving the techniques of separating the two oxides. Pure materials are now available for the determination of physical properties.

Both hafnia and zirconia undergo a monoclinic-to-tetragonal phase transformation at high temperatures. The transformation occurs over a temperature interval in the neighborhood of 1100°C for zirconia and approximately 1700°C for hafnia. The employment of zirconia and hafnia is severely restricted by volume contractions during the transformation which cause destruction of sintered bodies.

It is known that hafnia and zirconia can be transformed into a cubic crystal structure which is free of the destructive transformation by the addition of calcia, magnesia, or yttria. The cubic structure is similar to that of the

mineral fluorite and is commonly called "stabilized hafnia" or "flourite phase". It has been shown by Buckley and Wilder (1) that yttria-stabilized hafnia is more resistant to decomposition at high temperatures than either calcia- or magnesia-stabilized hafnia.

In addition to the nuclear applications suggested by the properties of pure hafnia, stabilized hafnia may be used as refractory containers or as oxidation-resistant coatings for metal surfaces (1,2). Schieltz (3) has found that yttria-stabilized hafnia is a solid electrolyte and as such may be used to measure oxygen concentrations in hot gases and liquid metals. Solid electrolytes are also used as fuel cells to produce small amounts of electric power.

The potential of yttria-stabilized hafnia has been demonstrated, but its employment is presently restricted by insufficient data on its high temperature properties. The present study was undertaken to provide information about the high temperature phase equilibria of the yttria-hafnia system, to measure the thermal expansion of the fluorite compositions throughout the complete phase domain, and to measure the axial thermal expansion of hafnia through the temperature interval of its monoclinic-to-tetragonal phase inversion.

# LITERATURE REVIEW

## Polymorphs of Hafnia

### Monoclinic phase

At room temperature, hafnia has a monoclinic crystal structure. The lattice parameters given by Adam and Rogers (4) are: a = 5.1156 A, b = 5.1722 A, c = 5.2948 A, and $\beta$ = 99° 11'. The unit cell contains four $HfO_2$ units and can be considered as a distorted cubic fluorite structure. Monoclinic hafnia has been found to be isomorphous with the room temperature form of zirconia (4,5). Complete solid solubility is observed in the hafnia-zirconia binary system (6).

### Monoclinic-to-tetragonal transformation

When monoclinic hafnia is heated to about 1700°C, it undergoes a nonquenchable transformation to the tetragonal phase. Wolten (7) has found that the transformation occurs over a temperature interval of about 150 C°. On cooling, the reverse transformation occurs at lower temperatures with hysteresis of 20 to 30 C°. At a constant temperature within the transformation interval, the relative proportions of the two phases do not change with time.

Wolten has compared the monoclinic-to-tetragonal transformation in hafnia to the diffusionless martensitic transformation in the cadmium-gold system. In a diffusionless transformation, all the atoms retain the same neighbors

making the new structure a distorted form of the initial one. Strain energy becomes a variable in the phase rule allowing the transformation to occur over a temperature interval instead of at a single temperature as is normally expected for a single compound.

Two grades of hafnia were used by Wolten (7) to determine the effect of purity on the transformation. The spectrographic material was of high purity except for 0.5% zirconium. The zirconium-free grade contained only 30 ppm zirconium but was less free of other impurities. The spectrographic grade was found to have a mean transformation temperature 100 $C^{o}$ lower than the zirconium-free grade. Wolten attributed the difference to the total impurities rather than to the zirconium content. The monoclinic-to-tetragonal transformation in zirconia was observed near 1000°C with a hysteresis of 200 $C^{o}$.

Ruh and Corfield (5) have proposed that the difference in transformation temperatures for hafnia and zirconia is due to the attainment of a critical metal-to-oxygen distance at the temperature of the transformation. By extrapolating the lattice parameters of Grain and Campbell (8), they were able to show that the lattice parameters of hafnia at 1700°C are close to those of zirconia at 1100°C. According to this theory, substituting larger cations for $Hf^{4+}$ increases the effective metal-to-oxygen bond distance making high temperature structures stable at lower temperatures.

Table 1. Transformation temperatures for the monoclinic-to-tetragonal phase transformation in hafnia

| Reference | M-to-T start (°C) | M-to-T end (°C) | T-to-M start (°C) | T-to-M end (°C) | Comments |
|---|---|---|---|---|---|
| Curtis *et al.* (10) | 1640 | 1920 | - | - | 99.8% $HfO_2$ (2 ppm Zr) Probably oxygen deficient (8) |
| Baun (9) | 1500 | 1600 | 1550 | 1450 | Spectrographic grade not oxygen deficient |
| Baun (9) | 1650 | 1900 | - | - | Spectrographic grade oxygen deficient |
| Wolten (7) | 1610 | 1770 | 1740 | 1550 | Zirconium-free grade |
| Wolten (7) | 1500 | 1690 | 1600 | 1460 | Spectrographic grade |
| Ohnysty and Rose (11) | 1593 | 1816 | 1638 | 1288 | From bulk thermal expansion nuclear grade |
| Stansfield (12) | 1840 | | 1790 | | 99.9% $HfO_2$ (180 ppm Zr) by dilatometry |
| Boganov *et al.* (13) | 1900 | 2000 | - | - | >99.8% $HfO_2$ |
| Ruh *et al.* (6) | 1620 | 1650 | 1620 | 1520 | 99.93% $HfO_2$ |
| Johnstone (14) | 1580 | 1825 | - | - | Spectrographic grade (64 ppm Zr) |

Baun (9) has determined the effect of oxygen deficiency on the monoclinic-to-tetragonal phase transformation in hafnia. Fresh samples not previously sintered in an oxygen deficient atmosphere transformed over the interval 1500° to 1600°C on heating. After the samples had been sintered at 1900°C in an oxygen deficient atmosphere, the transformation interval was raised to 1650°C to 1900°C. The interval found for oxygen deficient hafnia is in good agreement with the results of Curtis et al. (10) who, according to Baun, probably used oxygen deficient material.

A summary of temperature intervals for the monoclinic-to-tetragonal phase transformation of hafnia is given in Table 1. All determinations were made by high temperature X-ray diffraction except where noted.

Tetragonal phase

The tetragonal phase of hafnia has the following lattice constants at 1920°C according to Curtis et al. (10): a = 5.14 and c = 5.25. Isupova et al. (15) found the lattice parameters to be a = 5.175 and c = 5.325 at 2000°C. These results are in excellent agreement with those of Boganov et al. (13) who measured the thermal expansion of tetragonal hafnia in the temperature interval 2100° to 2725°C. Due to other similarities of the two oxides, Smith and Newkirk (16) believe tetragonal hafnia is isostructural with the tetragonal zirconia structure determined by Teufer (17). The tetragonal

structure may be considered as a slightly distorted fluorite structure.

Cubic phase

A high temperature cubic form of hafnia and zirconia has been reported by Boganov et al. (13). High temperature X-ray diffraction techniques were used to investigate materials containing less than 0.2% impurities. Cubic zirconia was found to be stable above 2300°C. The transformation was found to be reversible with no more than 30 C° hysteresis. The temperature of the formation of cubic hafnia was estimated to be 2700° to 2750°C. The results of Boganov et al. are in good agreement with the complete transformation of zirconia into the cubic phase above 2285°C as reported by Smith and Cline (18).

Engelke et al. (19) observed both monoclinic and cubic hafnia in hafnium carbide which had been plasma-sprayed in the presence of oxygen. Although the plasma-sprayed material undoubtedly contained impurities, Engelke et al. proposed the stabilization of hafnia into a fluorite-type defect structure by reduction rather than the introduction of a second oxide.

## Polymorphs of Yttria

Cubic phase

At room temperature yttria exists in the body-centered cubic thallium oxide structure which is also known as the

rare earth oxide C structure. The cell contains 16 $Y_2O_3$ units (20). Atomic positions can be found in International Tables for X-ray Crystallography (21). The unit cell of the thallium oxide structure is not unlike a cube made of 8 fluorite unit cells where 1/4 of the oxygen positions are unoccupied. The distortion in the remaining atomic positions gives thallium oxide a body-centered cubic lattice and a unit cell parameter about twice that of the fluorite structure.

Hexagonal phase

At very high temperatures, the thallium oxide structure of yttria transforms into a hexagonal structure designated as the rare earth oxide H structure. The temperature of the transformation has been given by Foex and Traverse (22) as about 2250°C. The temperature of the transformation is presented as 2300°C on the zirconia-yttria phase diagram by Rouanet (23).

## Yttria-Hafnia Fluorite Phase

It is found that the addition of calcia, magnesia, yttria, or rare earth oxides to hafnia produces a cubic structure (1,14). The structure is like that of the mineral fluorite ($CaF_2$) and is thus called the yttria-hafnia fluorite phase or stabilized hafnia.

Several attempts have been made to define the extent of the fluorite phase region in the yttria-hafnia system.

According to Besson et al. (24) who used dry mixed yttria-hafnia compositions fired at 1800°C for 4 hours, the fluorite phase extends from 8 to beyond 40 mole % yttria. Using similar preparation techniques, Caillet et al. (25) observed the fluorite phase from 8 to 45 mole % yttria at 1800°C. Caillet et al. investigated compositions containing up to 50 mole % yttria.

Isupova et al. (15) has determined the phase diagram in the hafnia-rich region of the yttria-hafnia system. The lower limit of the fluorite phase was found to be 10 mole % yttria at 1300°C, 7 mole % yttria at 1500°C, 3 mole % yttria at 1800°C, and 5 mole % yttria at 1900°C.

It has been observed by Buckley and Wilder (1) that long anneals at high temperatures are required to achieve stabilization of hafnia with yttria additions if the two oxides are dry mixed. Nine hours at 2000°C was required to completely stabilize a composition of 11 mole % yttria. Yttria was found to be superior to calcia and magnesia for stabilizing hafnia at high temperatures.

## Nonexistence of Yttria-Hafnia Pyrochlore

The existence of a pyrochlore in some rare earth oxide-zirconia compositions (26) suggested the possibility of the formation of such a phase of composition $Y_2O_3$-$2HfO_2$. At this composition, a unit cell of the fluorite structure contains

two $HfO_2$ units and one $Y_2O_3$ unit. The oxygen sublattice has one unoccupied position. Ordering of $Hf^{4+}$ and $Y^{3+}$ on the cation sublattice and the vacant oxygen site on the oxygen sublattice would create the pyrochlore structure. Pyrochlore has a body-centered cubic lattice and a lattice parameter twice that of the fluorite phase. A detailed discussion of the pyrochlore phase has been given by Roth (26).

The X-ray diffraction study of Perez y Jorba (27) on a coprecipitate of composition $Y_2O_3$-$2HfO_2$ showed the nonexistence of pyrochlore in the yttria-hafnia system. Komissarova et al. (28) confirmed the results of Perez y Jorba using coprecipitated material calcined at 1300°C. Additional evidence for the nonexistence of yttria-hafnia pyrochlore is the neutron diffraction study of Smith (29) showing the absence of pyrochlore in the yttria-zirconia system.

## Thermal Expansion Measurements

### Hafnia

The axial thermal expansion of monoclinic hafnia has been measured by Grain and Campbell (8), Patil and Subbarao (30), and Filatov and Frank-Kamenetskii (31). The results of these studies are included in Figures 17, 18, and 19. The length of the monoclinic b axis remains nearly constant from room temperature to about 800°C. Then it increases only slightly as the temperature is increased to 1400°C. The

length of the monoclinic a and c axes increase continuously over the complete temperature interval while the $\beta$ angle decreases slightly.

The axial thermal expansion of tetragonal hafnia from 2100° to 2725°C has been measured by Boganov et al. (13). The tetragonal lattice parameters measured by Isupova et al. (15) at 2000°C agree with the results of Boganov et al. No report was found in the literature containing the thermal expansion of hafnia through the temperature interval of the monoclinic-to-tetragonal phase transformation.

Yttria

The thermal expansion of yttria has been measured by Stecura and Campbell (32) using high temperature X-ray diffraction. See Figure 13. Wilfong et al. (33) measured the thermal expansion of yttria by interferometric technique. Calderwood[1] and Stacy (34) used yttria of the same purity but different dilatometers to study thermal expansion. A summary of the thermal expansion data for yttria is presented in Figure 14.

---

[1]Calderwood, F. W., Ames Laboratory, Ames, Iowa. Thermal expansion of yttria. Private communication. 1970.

Yttria-hafnia fluorite

Caillet et al. (25) used a dilatometer to measure the thermal expansion of yttria-hafnia fluorite specimens of composition 12 to 40 mole % yttria. The thermal expansion coefficient of each specimen was constant between 800° and 1400°C. A maximum was observed in the thermal expansion coefficient at 33.3 mole % yttria. Caillet et al. present the appearance of the maximum in thermal expansion as partial evidence of a pyrochlore compound in the yttria-hafnia system.

Ohnysty and Rose (11) have measured the thermal expansion of hafnia stabilized with 8.5 and 12.3 mole % yttria. The measurements were made from room temperature to 980°C with a dilatometer and from 980° to 2480°C in an apparatus where the thermal expansion of the sample is compared to that of tungsten.

A recent literature review on hafnia has been compiled by Lynch (35).

# EXPERIMENTAL PROCEDURE

## Materials

The yttria used in this study was supplied by the Ames Laboratory as clinker from the calcination of hydrated yttrium oxalate. An emission spectrographic analysis of the impurities is given in Table 2.

Table 2. Emission spectrographic analysis of yttria

| Element | Concentration (ppm) |
|---|---|
| Ca | 20 |
| Mg | 20 |
| Si | 200 |
| Fe | 35 |
| Na | faint trace |
| Cu | 20 |
| Ti | 30 |
| Ta | <200 |
| Al | 100 |
| Co | 35 |
| Yb | <100 |
| Er | <100 |
| Ho | 60 |
| Dy | <100 |
| Gd | <100 |
| Tb | <200 |
| Sm | <250 |
| Total | <1570 |

The hafnia was obtained from Wah Chang Corporation (Albany, Oregon) as spectrographic grade hafnium oxychloride

(Lot SP 10684B). The emission spectrographic analysis supplied by the manufacturer is given in Table 3.

Table 3. Emission spectrographic analysis of hafnium oxychloride

| Element | Concentration (ppm) |
|---|---|
| Al | 25 |
| B | 0.2 |
| Cb | 100 |
| Cd | 1 |
| Co | 5 |
| Cr | 10 |
| Cu | 40 |
| Fe | 50 |
| Mg | 10 |
| Mn | 10 |
| Mo | 10 |
| Ni | 10 |
| Pb | 5 |
| Si | 40 |
| Sn | 10 |
| Ta | 200 |
| Ti | 20 |
| V | 5 |
| W | 20 |
| Zr | 64 |
| Total | 635.2 |

The thoria ($ThO_2$) used as a thermal expansion reference was obtained from Zircoa Corporation of America (Solon, Ohio). The thoria was received as a sintered disk and was ground to -325 mesh for X-ray diffraction analysis. The spectrographic analysis supplied by Zircoa is given in Table 4.

Table 4. Emission spectrographic analysis of thoria

| Element | Concentration (ppm) |
|---|---|
| Al | 30 |
| Sb | ND[a] |
| As | ND |
| Ba | ND |
| Be | ND |
| Bi | ND |
| B | ND |
| Cd | ND |
| Ca | 100 |
| Cr | 10 |
| Co | 80 |
| Cu | 10 |
| Fe | 3 |
| Pb | ND |
| Mg | 1 |
| Mn | <1 |
| Mo | <1 |
| Ni | 80 |
| P | ND |
| Si | 100 |
| Ag | <1 |
| Sr | ND |
| Sn | ND |
| Ti | ND |
| V | ND |
| Zn | ND |
| Zr | 200 |
| Total | <617 |

[a]Not detected.

## Sample Preparation

Standard solutions were prepared for the coprecipitation of yttria-hafnia compositions. The yttria clinker was dissolved in boiling concentrated hydrochloric acid. The solution was diluted with distilled water to reduce the acid concentration to 4N and the yttria concentration to 0.0489 gm./ml. The yttria concentration was obtained by averaging 7 gravimetric determinations. The second solution was prepared by dissolving hafnium oxychloride in distilled water. The hafnia concentration of the solution was found to be 0.0958 gm./ml. by averaging 6 gravimetric determinations.

Yttria-hafnia compositions were prepared by coprecipitating hafnium and yttrium hydroxides. Desired proportions of the two standard solutions were pipetted into a Pyrex beaker. Care was taken always to add the hafnia solution to the yttria solution to maintain maximum acid concentration during mixing. The mixture was stirred for 15 minutes and slowly added to excess 10N ammonium hydroxide. The ammonium hydroxide was agitated with a magnetic stirrer during the addition of the mixed solutions and for several minutes afterward. Pure hafnia samples were prepared by precipitating only hafnium hydroxide.

The gelatinous hydrated hydroxide precipitates (36) were filtered, washed, and dried overnight at 110°C in the filter paper. The dry precipitates were then transferred to

porcelain crucibles, partially covered, and calcined in a muffle furnace for at least one hour at 1000°C.

The calcined clinker was ground to -325 mesh with a Diamonite mortar and pestle (Diamonite Products Manufacturing Co., Shreve, Ohio). The powder was pressed to 900 p.s.i. in a 3/8 in. diameter double-acting steel die. The pellets were then isostatically pressed to 50,000 p.s.i. Pellets were placed in a covered yttria crucible for annealing. Small chips of material of similar composition were used to separate the pills within the crucible.

High temperature anneals were performed in a resistance furnace with tungsten heating element (Centorr Associates, Inc., Suncook, New Hampshire). A continuously flowing atmosphere of argon protected the element from oxidation. Temperatures were measured with a calibrated optical pyrometer (Leeds & Northrup Co., Philadelphia, Pennsylvania). Black body conditions were assumed for the furnace arrangement.

Pellets were annealed for 4 hours at 1500° and 1600°C and 2 hours at 1900°, 2000°, and 2200°C. Additional anneals of 8 hours at 1600°C and 4 hours at 2000°C were made on compositions close to observed phase boundaries. Pellets were cooled in the furnace as rapidly as possible (about 6 minutes from 2000° to 600°C).

Cooled pellets were of varying shades of grey or black

depending on the temperature and duration of the high temperature anneals indicating that partial reduction had occurred (37). The pellets could have been reoxidized by heating at 1000°C for several hours. However, no difference was observed in X-ray diffraction patterns of the reduced and reoxidized specimens.

Wet chemical analyses were performed on several coprecipitated compositions. Two sample sizes were used. Typical results on 1/2 gm. samples are given in Table 5.

Table 5. Chemical analysis of yttria-hafnia compositions

| Calculated composition (mole % yttria) | Composition from chemical analysis (mole % yttria) |
|---|---|
| 28 | 28.2 |
| 32 | 32.0 |
| 33.3 | 33.5 |
| 37 | 36.8 |

Chemical analyses performed on 1/10 gm. samples were inconclusive because of poor mass balance. In all cases, the compositions were assumed to be as calculated from the volumes of standardized solutions mixed together for the coprecipitation.

Some typical microstructures of yttria-hafnia compositions are shown in Figures 1 and 2. The materials were

5 m/o $Y_2O_3$ - 95 m/o $HfO_2$ 2000°C - 2 hrs. 25 min. hot phosphoric acid etch 320X fluorite + Mss

40 m/o $Y_2O_3$ - 60 m/o $HfO_2$ 2000°C - 2 hrs. 7 min. hot phosphoric acid etch 320X fluorite

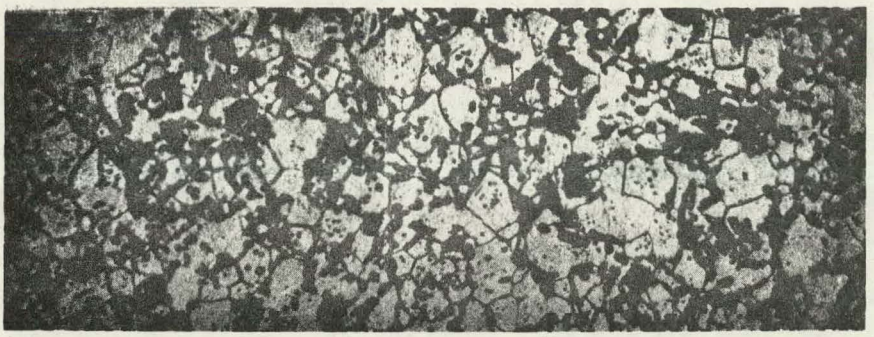

52 m/o $Y_2O_3$ - 48 m/o $HfO_2$ 2200°C - 2hrs. 2 min. hot phosphoric acid etch 320X fluorite

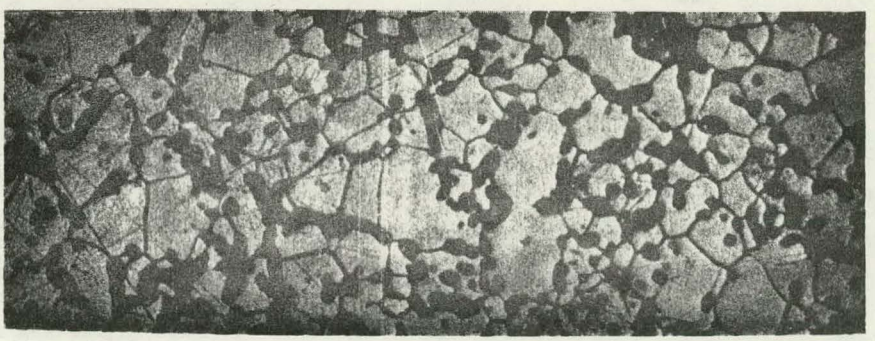

Figure 1. Microstructures of yttria-hafnia compositions

58 m/o $Y_2O_3$ - 42 m/o $HfO_2$ 2200°C - 2 hrs. 2 min. hot phosphoric acid etch 320X fluorite + Yss

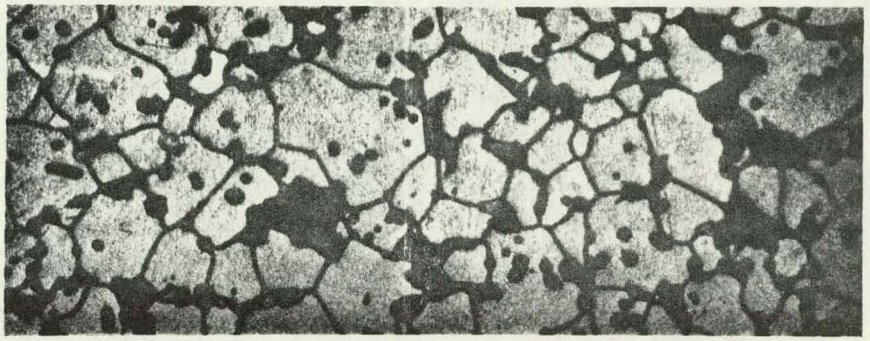

70 m/o $Y_2O_3$ - 30 m/o $HfO_2$ 2000°C - 2 hrs. 15 sec. hot phosphoric acid etch 800X fluorite + Yss

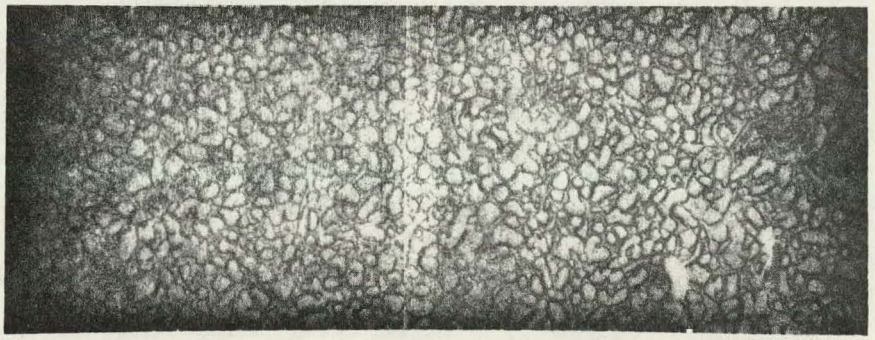

95 m/o $Y_2O_3$ - 5 m/o $HfO_2$ 2000°C - 2 hrs. 8 sec. hot phosphoric acid etch 320X Yss

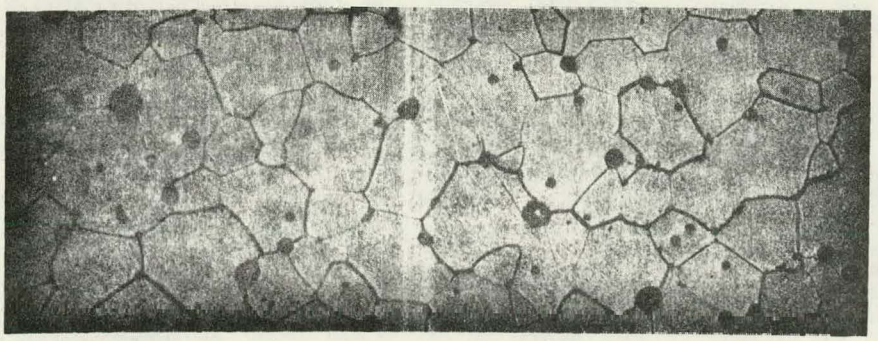

Figure 2. Microstructures of yttria-hafnia compositions

mounted in mineral filled diallyl phthalate (Buehler Ltd., Evanston, Illinois). This mounting material was chosen because of its resistance to hot phosphoric acid (38). Polishing was done with 600 mesh silicon carbide paper and cloth laps using 0.3 micron Alpha Micropolish and 0.05 Gamma Micropolish (Buehler Ltd., Evanston, Illinois). Etching times with hot phosphoric acid are listed in the captions of Figures 1 and 2.

The apparent density of fluorite compositions was determined by the water displacement technique (39). Two sintering schedules were used. Specimens of composition 6 to 20 mole % yttria were sintered at 2000°C for 1 hour with an additional 30 minute anneal at 1500°C (3). Specimens of composition 25 to 50 mole % yttria were sintered at 1600°C for 4 hours. As can be seen in the microstructures, the pellets are very porous. Assuming most of the pores are open, the apparent density is a good approximation of the true density. Specimen surfaces were cleaned with 240 mesh silicon carbide paper before density measurements were made.

## Room Temperature X-ray Diffraction Analysis

Room temperature phase identification and lattice parameter measurements were made on annealed pellets. The pellets were polished on one face with 500 mesh silicon carbide paper and mounted polished face up on a glass slide

with modeling clay. The face of the pellet was made parallel to the slide using a micrometer as a clamp. The glass slide was mounted in the diffractometer for X-ray analysis. Room temperature X-ray diffraction analyses were performed on a Norelco Wide Range Diffractometer with Mark III Data Control (Philips Electronic Instruments, Mount Vernon, New York). The scan rate was $1^{\circ}$ $2\theta$/min. in the direction of increasing $2\theta$. Nickel filtered copper radiation, $1^{\circ}$ divergent and anti-scatter slits, and a 0.003 in. receiving slit were used.

Precise lattice parameters were calculated using the extrapolation function $\cos\theta \cot\theta$ of the computer program by Vogel and Kempter (40) as modified to include the monoclinic problem[1]. Both $CuK_{\alpha_1}$ and $CuK_{\alpha_2}$ reflections greater than $60^{\circ}$ $2\theta$ were used in calculating precise lattice parameters of the fluorite and yttria solid solution phases. Lattice parameters determined from Debye-Scherrer powder patterns agreed well with those calculated from diffractometer data.

Cooled specimens were assumed to maintain the high temperature structure except where the monoclinic-to-tetragonal phase transformation of hafnia solid solutions were involved. Since the tetragonal phase could not be

---

[1]Smith, J. and Bowman, A., Los Alamos Scientific Laboratory, Los Alamos, New Mexico. Unpublished modification to Vogel-Kempter lattice parameter program to include monoclinic problem. Private communication to Mr. John Mason. 1964.

quenched in, any tetragonal phase present at high temperatures would be detected as monoclinic phase at room temperature. The monoclinic-to-tetragonal phase transformation was studied by high temperature X-ray diffraction.

## High Temperature X-ray Diffraction Analysis

High temperature X-ray diffraction studies were made with a MRC X-86-N3 high temperature diffractometer attachment (Materials Research Corporation, Orangeburg, New York) mounted an a Norelco Wide Range Diffractometer. The attachment consists of a specimen stage of heater electrodes and alignment gearing contained in a water-cooled vacuum chamber. The chamber has two 10 mil beryllium windows which allow the incident and diffracted beams to pass with minimum absorption. The chamber cover is fitted with a vacuum port and a fused quartz window which allows the specimen to be observed with an optical pyrometer. Electrical power is supplied to the attachment through water-cooled cables. The power supply was operated on rheostat control because of the high temperatures required. The electrode clamps and screws supplied by the manufacturer were made of brass. These were replaced by copper parts to increase thermal conductivity and prevent the contamination of the system by volatilized zinc.

The vacuum system consisted of a liquid nitrogen cold trap, air-cooled diffusion pump, and mechanical vacuum pump which was mounted separately to reduce vibrations to the

diffractometer attachment. The vacuum system was attached to the port on the chamber cover by a flexible stainless steel bellows. Vacuums of $5 \times 10^{-5}$ torr were routinely achieved.

The combination specimen holders and heating elements were fabricated of ductile 2 mil tungsten 5/16 in. wide and 1 1/4 in. long (H. Cross Company, Weehawken, New Jersey). Both ends of the heating elements were bent at right angles leaving a 3/8 in. long platform onto which the specimen was placed. A new heating element was required for each composition.

Materials used for high temperature X-ray diffraction studies were annealed at high temperatures to promote crystal growth. This was necessary to avoid line broadening at the lower temperatures of thermal expansion runs (41). Yttria was hot pressed at 1600°C for 15 minutes at 3300 p.s.i. Hafnia was annealed 1 hour at 1900°C and 2 mole % yttria-hafnia was annealed 2 hr. at 1900°C 8, 14, 20, and 33.3 mole % yttria-hafnia fluorite compositions were sintered at 2000°C for 1 hour followed by 30 minutes at 1500°C (3). 30, 40, and 50 mole % yttria fluorite compositions were annealed at 1600°C for 4 hours. The thoria had been sintered by the manufacturer. All materials were ground to -325 mesh for analysis.

When materials were examined by high temperature X-ray diffraction, each specimen was applied to the tungsten heater

before the heater was installed in the high temperature diffraction attachment. A slurry of a few milligrams of -325 mesh material was mixed with a saturated solution of Carbowax 4000 (Carbide and Carbon Chemical Co., New York, New York) in distilled water. The slurry was applied evenly to the heater with a small camel hair brush. Care was taken to keep the specimen within the hot zone of the heater. The wax slurry was allowed to dry at room temperature. Lines were scribed through the specimen with a razor blade to prevent the specimen from breaking loose from the heater because of thermal expansion differences. A small area about 2 millimeters square at the specimen center was cleared of material to provide a tungsten surface for the sighting of the optical pyrometer.

The heater with specimen coating applied was installed in the high temperature diffractometer attachment using the alignment jig provided by the manufacturer. The alignment was tested by scanning through a few diffraction peaks. The wax was burned off in air. Care was taken not to heat the tungsten hot enough to cause serious oxidation. It was found that the specimen remained in alignment throughout the high temperature runs.

Lattice parameters were measured in the temperature interval 900° to 1950°C in order to determine thermal expansion. The temperature of the high temperature X-ray diffrac-

tion specimen was increased by adjusting the rheostat on the power supply. Fifteen minutes were allowed for the specimen to achieve constant temperature. The temperature of the heating element was measured with the optical pyrometer. For specimens of thoria, yttria, and yttria-hafnia fluorite compositions, all peaks within the interval $50^{\circ}$ to $130^{\circ}$ $2\theta$ were scanned in direction of increasing $2\theta$. The diffraction peaks in the interval $20^{\circ}$ to $60^{\circ}$ $2\theta$ were scanned for monoclinic and tetragonal hafnia. After the peaks were scanned at a given temperature setting, the temperature was reread. Since the lattice parameters were determined by extrapolation and the peaks were always scanned in the direction of increasing $2\theta$, the final temperature was used in plotting thermal expansion curves. In most cases, the variation of temperature during the scan was only a few degrees.

For phase identification in studying the monoclinic-to-tetragonal phase transformations in hafnia and 2 mole % yttria-hafnia, only the low $2\theta$ angles containing the $\{111\}$ and $\{200\}$ peaks were scanned.

Temperatures were measured with a disappearing filament micro-optical pyrometer (Pyrometer Instrument Company, Inc., Bergenfield, New Jersey). Since the angle of observation with the heater surface was approximately $50^{\circ}$ from normal, normal emissivity corrections for tungsten could not be applied (42, page 131). The micro-optical pyrometer readings

were calibrated against melting points of standard materials. The pyrometer was focused on the tungsten heater adjacent to a small amount of the standard material. The temperature was increased slowly and the observed melting temperature of the standard was noted. A temperature calibration curve was constructed using the data of Table 6.

Table 6. Calibration points of the micro-optical pyrometer for the X-ray furnace attachment

| Material | Observed apparent melting point °C | True melting point °C (43) |
|---|---|---|
| Au | 989<br>990<br>993 | 1063 |
| Ni | 1335<br>1328<br>1328<br>1335 | 1453 |
| Pd | 1419<br>1400<br>1380<br>1410 | 1552 |
| Pt | 1615<br>1590<br>1612<br>1597 | 1769 |
| Rh | 1785<br>1775<br>1790<br>1796<br>1760<br>1772 | 1960 |
| $Al_2O_3$ | 1835<br>1835 | 2040 |

Since the observed melting points were made under experimental conditions, a correction for the fused quartz sight glass was included. Care was taken during the course of experiments to maintain the same pyrometer position as was used for calibration.

## Liquidus Temperature Measurement

Liquidus temperatures of yttria-hafnia compositions were determined in a water-cooled copper furnace which used a 2 mil tungsten element as heater and sample support. Figure 3 is a schematic drawing of the furnace. Power was supplied by a variable transformer in series with a high-current transformer with secondary rating of 10 volts and 500 amps. The maximum power used was 1 Kva for a temperature of 2900°C.

Temperatures were measured with the micro-optical pyrometer used in high temperature diffraction studies. Since the pyrometer was positioned perpendicular to the heater surface, it was appropriate to use the normal spectral emissivity of tungsten (44) for temperature corrections. Using the emissivity corrections for tungsten and experimentally determined correction factors for the absorption of the quartz window, a calibration curve was constructed. As an independent check on the calibration curve, the melting points of several refractory materials were determined and compared with literature values. Table 7 shows the agreement of experimentally determined melting points (average corrected

Figure 3. Schematic drawing of melting point furnace

A. Fused quartz sight port; eccentric mount
B. Copper housing
C. O-ring seal
D. Vacuum port
E. Water cooled electrodes
F. Copper blocks for clamping heating elements
G. Tungsten heating element/sample support
H. Radiation shields
I. Electrical insulating vacuum seal
J. Cooling coils
K. Sight port shutter
L. Sight port shutter control knob

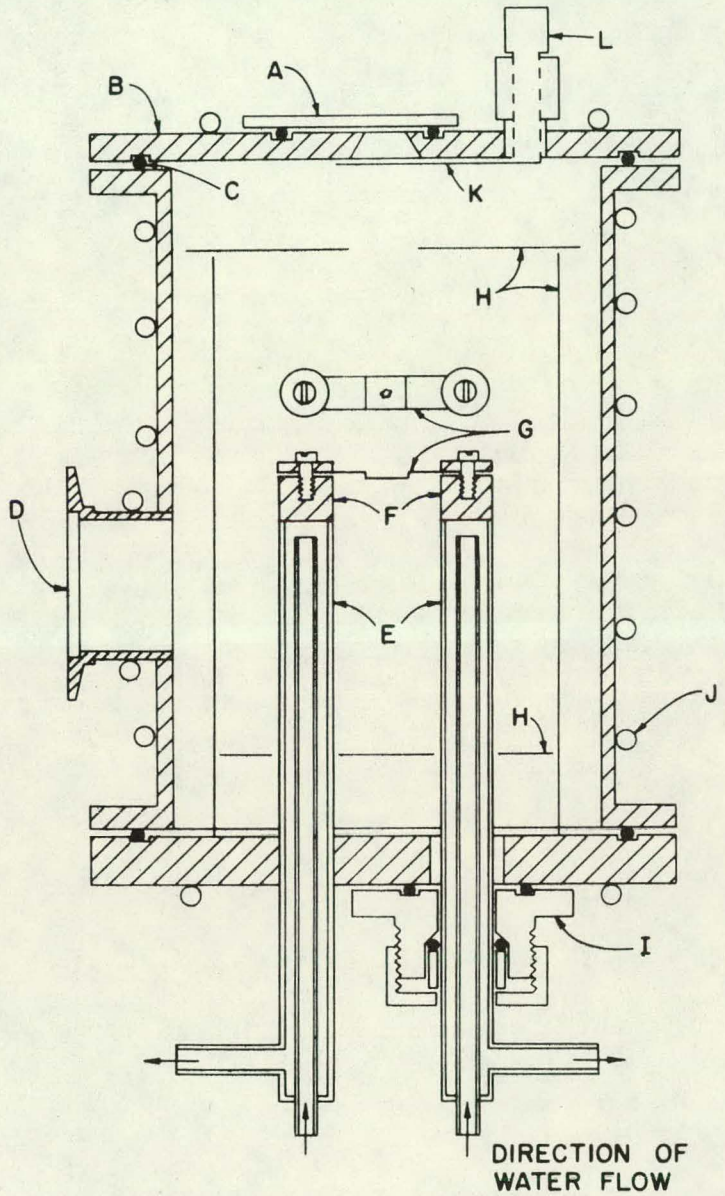
L
A
B
C
K
H
G
F
D
E
H
J
I
DIRECTION OF
WATER FLOW

Table 7. Melting points of refractory materials measured with melting point apparatus and compared to literature values

| Material | Observed temp. (°C) | Corrected temp. (°C) | Average corrected temp. (°C) | Literature values (45) (°C) |
|---|---|---|---|---|
| $Al_2O_3$ | 1838 | 2033 | | 2040- |
| | 1838 | 2033 | 2029 | 2050 |
| | 1822 | 2020 | | |
| $Y_2O_3$ | 2142 | 2412 | | 2410- |
| | 2137 | 2407 | 2410 | 2420 |
| Ir | 2158 | 2433 | | |
| | 2170 | 2447 | | |
| | 2182 | 2460 | 2444 | 2443 |
| | 2163 | 2438 | | |
| | 2168 | 2440 | | |
| Mo | 2315 | 2635 | | |
| | 2290 | 2602 | | 2610- |
| | 2308 | 2625 | 2621 | 2630 |
| | 2303 | 2620 | | |
| | 2306 | 2623 | | |
| $ZrO_2$ | 2365 | 2703 | | |
| | 2354 | 2689 | | 2677- |
| | 2366 | 2705 | 2687 | 2722 |
| | 2338 | 2670 | | |
| | 2338 | 2670 | | |

temperature) and values reported in the literature.

Melting points of yttria and hafnia and the liquidus temperatures of yttria-hafnia compositions were determined by visual observation through the micro-optical pyrometer. A few milligrams of the material to be studied were deposited on the heating element. The element was heated slowly under

vacuum until flow of the material was observed. As can be seen in Table 7, this technique gave reproducible results for congruently melting materials.

# RESULTS AND DISCUSSION

## Monoclinic-to-Tetragonal Phase Transformation

The monoclinic-to-tetragonal phase transformation of hafnia was studied by high temperature X-ray diffraction. The temperature interval in which the monoclinic and tetragonal phases coexist was found to be 1750° to 1850°C on heating and 1800° to 1550°C on cooling. The reported temperatures were determined by averaging the results of six separate determinations. The standard deviation of the reported temperatures is 55C°. The large value of the standard deviation found in this study and the variation of the temperature intervals of the transformation found in the literature (Table 1) indicate that the factors which affect the transformation are not easily controlled.

As has been discussed by Baun (9), oxygen deficiency has a large effect on the temperature of the transformation. The hafnia used to determine the temperature interval was probably oxygen deficient. The starting material had been sintered at 1900°C for one hour in argon and the transformation was studied under vacuum. For this reason, the temperature intervals determined are likely characteristic of oxygen deficient hafnia. Typical high temperature X-ray diffraction patterns showing the monoclinic-to-tetragonal phase transformation of hafnia are presented in Figure 4.

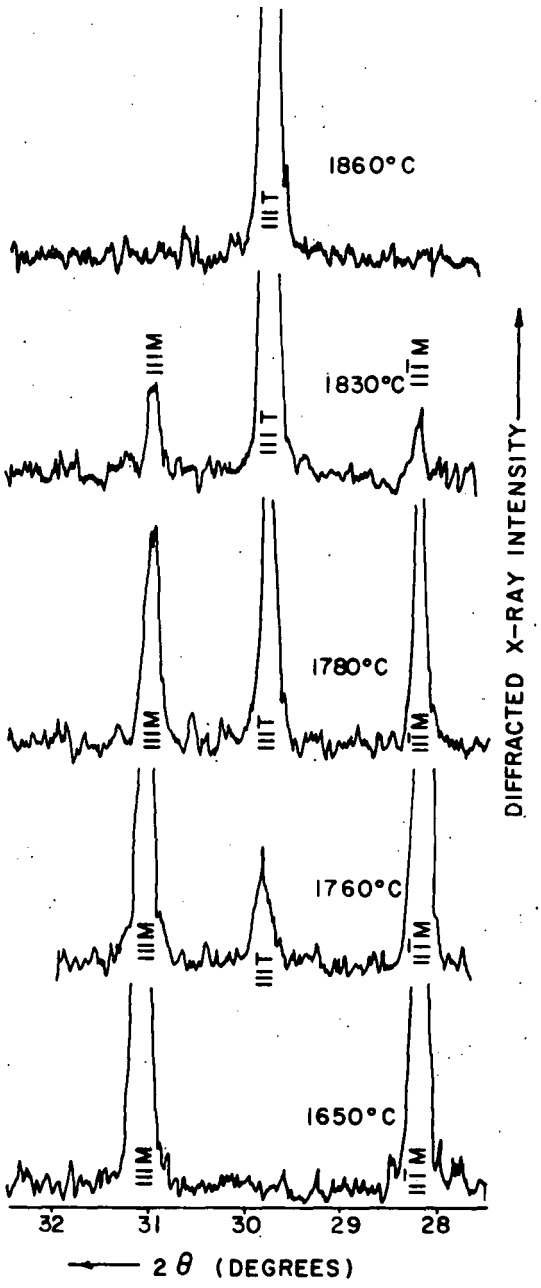


Figure 4. High temperature X-ray diffraction patterns of hafnia showing monoclinic-to-tetragonal phase transformation on heating

At 1650°C only the monoclinic phase is present. The start of the transformation is made evident at 1760°C by the appearance of the tetragonal 111 peak. As the temperature is increased, the relative intensity of the tetragonal peaks increases at the expense of the monoclinic peaks. At 1860°C the transformation is complete and the monoclinic peaks are not observed. Similar diffraction patterns were obtained at lower temperatures on cooling.

Below 2000°C, the solubility of yttria in hafnia is less than 1 mole % yttria. The monoclinic-to-tetragonal phase transformation of the limiting hafnia solid solution was observed in the presence of the fluorite phase in a 2 mole % yttria-hafnia composition. Diffraction patterns were similar to those obtained with pure hafnia with the addition of fluorite peaks at all temperatures. Interference of the 111 fluorite peak and the 111 tetragonal peak made it necessary to observe the 200 tetragonal peak to detect the formation of the tetragonal phase.

The temperature interval of the monoclinic-to-tetragonal transformation in the hafnia solid solution was found to be 1350° to 1750°C on heating and 1425° to 1200°C on cooling. Again the standard deviation of the temperatures for two determinations was about 50°C indicating the temperature interval is difficult to define precisely. Figure 5 shows the temperature interval of the monoclinic-to-tetragonal phase

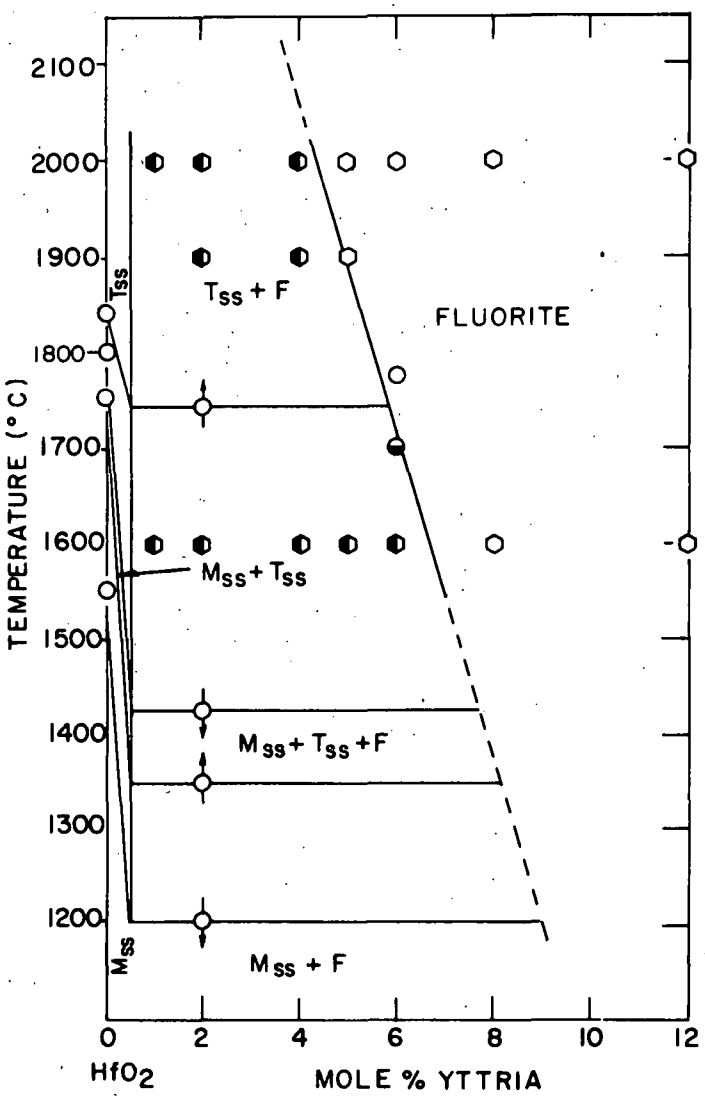


Figure 5. Hafnia-rich region of tentative yttria-hafnia phase diagram

transformation in pure hafnia and hafnia solid solution. The arrows through the data points indicate the intervals on heating and cooling.

The decrease in transformation temperature by the substitution of yttria into the hafnia lattice is in agreement with the results of other authors (9, 14, 15). According to Ruh and Corfield (5), the temperature of the transformation is controlled by the attainment of a critical oxygen-to-metal distance in the monoclinic structure. The introduction of the large yttrium ion into the lattice increases the effective metal-to-oxygen distance thus requiring less thermal expansion to achieve the critical distance at which the monoclinic phase is unstable. Likewise, the increase in transformation temperature caused by impurities in hafnia which has been reported by Wolten (7) could be explained if the impurity cations were smaller than hafnium.

## Phase Domains in the Yttria-Hafnia System

Phase domains in the yttria-hafnia system were determined from X-ray diffraction studies of annealed specimens which had been cooled rapidly to room temperature. Specimens were annealed for 4 hours at 1500° and 1600°C and for 2 hours at 1900°, 2000°, and 2200°C. Additional anneals were made on compositions close to observed phase boundaries for 8 hours at 1600°C and 4 hours at 2000°C. Phase boundaries

determined from specimens subjected to the longer anneals were identical to results obtained from specimens annealed for shorter times. The rate of cooling the specimens from 2000° to 600°C in about 6 minutes was sufficiently rapid to prevent any appreciable change in concentration by diffusion (46). It was therefore assumed that in all cases, except for the tetragonal phase of hafnia and hafnia solid solutions, the high temperature phases were retained at room temperature. On the basis of chemical analyses and the technique used in coprecipitating specimens, the compositions were considered to be within 0.5 mole % of the reported value.

Figure 6 shows room temperature X-ray diffraction patterns of hafnia-rich specimens annealed at 1600°C for 4 hours. The appearance of the 111 fluorite peak in the pattern of 1 mole % yttria-hafnia indicates that the solubility of yttria in hafnia is limited to less than 1 mole %. From 1 mole % yttria to 6 mole % yttria, a yttria solid solution + fluorite domain exists. At 8 mole % yttria, only the fluorite phase exists. The limits of the hafnia solid solution + fluorite domain at 1600°, 1900°, and 2000°C are shown on Figure 5. The lower composition boundary of the fluorite phase agrees well with that determined by Isupova *et al.* (15). However the interpretation of the phase diagram in the hafnia solid solution + fluorite domain is quite different.

As is shown in Figure 5, the lower boundary of the

Figure 6. Room temperature X-ray diffraction patterns of yttria-hafnia compositions showing stabilization with increased yttria content

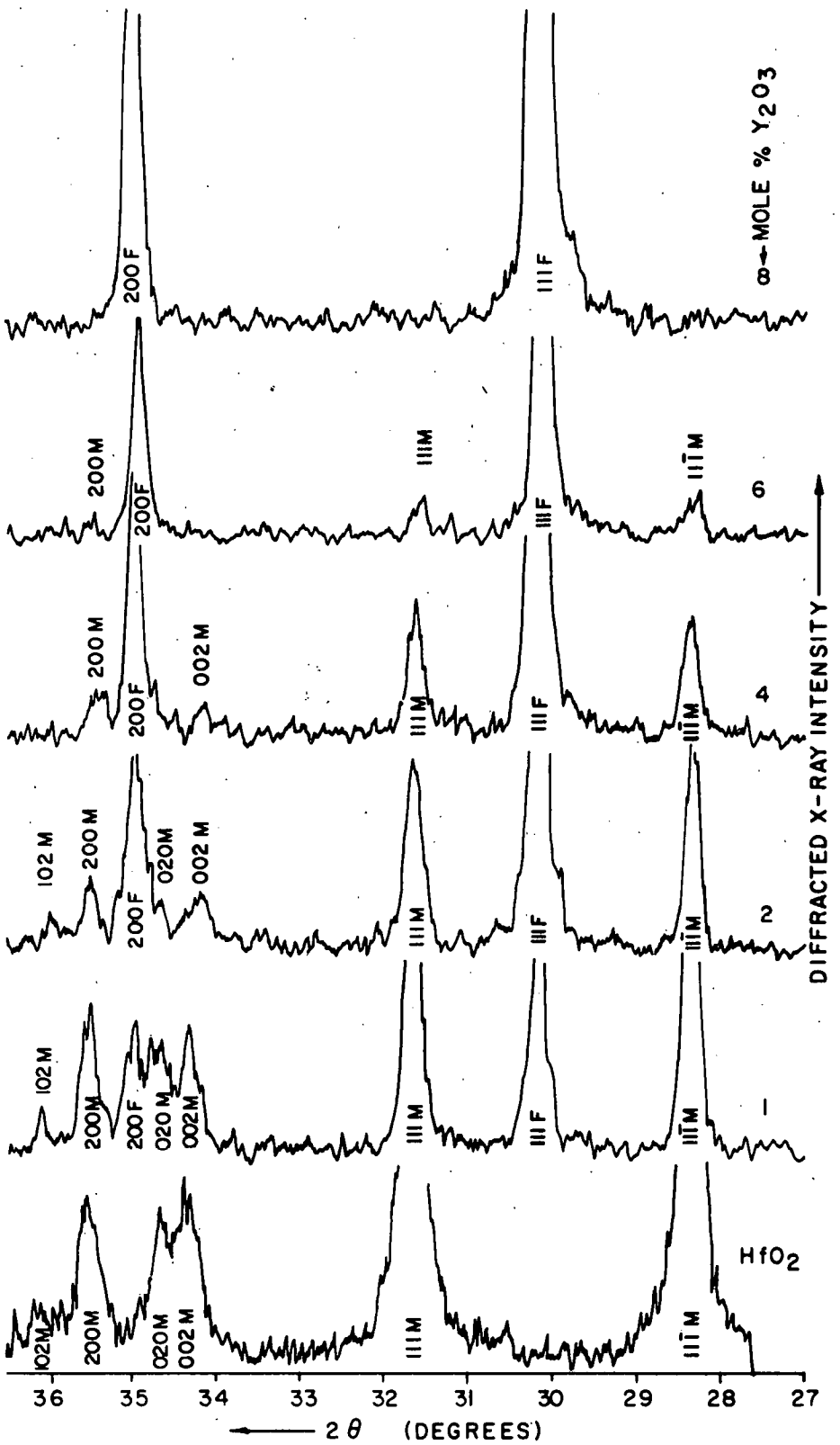
8 → MOLE % $Y_2O_3$
6
4
2
1
$HfO_2$
200F
111F
200M
111M
111̄M
002M
102M
020M
DIFFRACTED X-RAY INTENSITY
36
35
34
33
32
31
30
29
28
27
2θ (DEGREES)

fluorite phase was confirmed by high temperature X-ray diffraction. A specimen of 6 mole % yttria was annealed at 1700°C. The diffraction pattern included small, well defined $11\bar{1}$ and 111 monoclinic peaks. After a 2 hour anneal at 1775°C the diffraction pattern contained only peaks of the fluorite phase.

As is shown in Figure 6, the lower boundary of the fluorite domain is easily detected by observing the disappearance of the $11\bar{1}$ and 111 monoclinic peaks. However, the upper limit of the fluorite domain is not as easily determined. Figure 7 shows typical room temperature X-ray diffraction patterns of fluorite and yttria solid solution phases annealed at 1600°C. It is seen by observing the diffraction pattern of 60 mole % yttria that the major peaks of the yttria solid solution pattern interfere with the fluorite peaks making their first appearance difficult to detect.

The location of the upper boundary of the fluorite phase was determined by measuring the lattice parameters of fluorite compositions. As the yttria content was increased, the lattice parameter of the fluorite phase increased until the upper boundary of the domain was reached. When the two phase domain was entered, the composition of the fluorite phase remained constant and thus the lattice parameter remained constant. See Figure 8 and Appendix A. This technique was

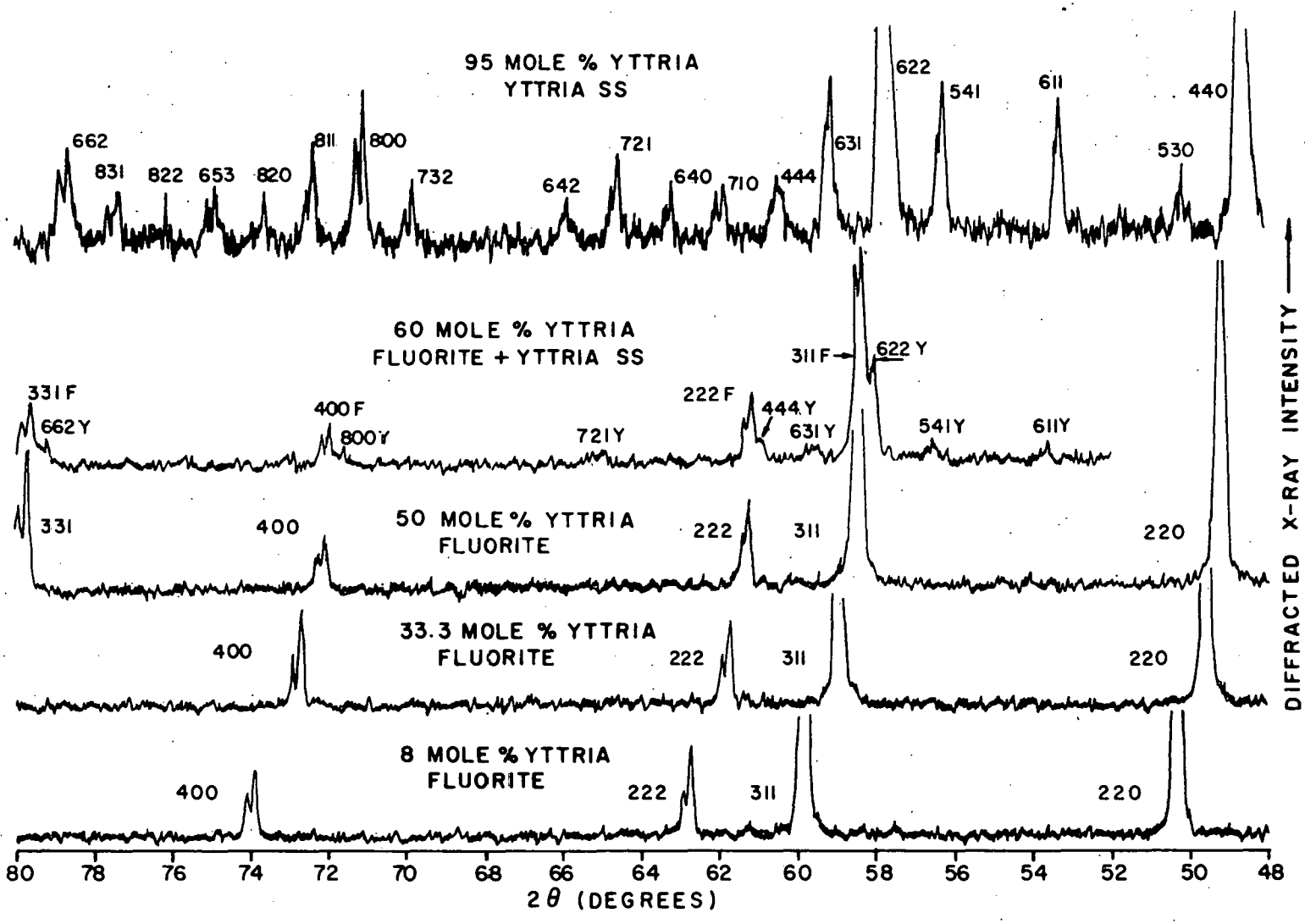


Figure 7. Room temperature X-ray diffraction patterns of fluorite and yttria solid solution phases

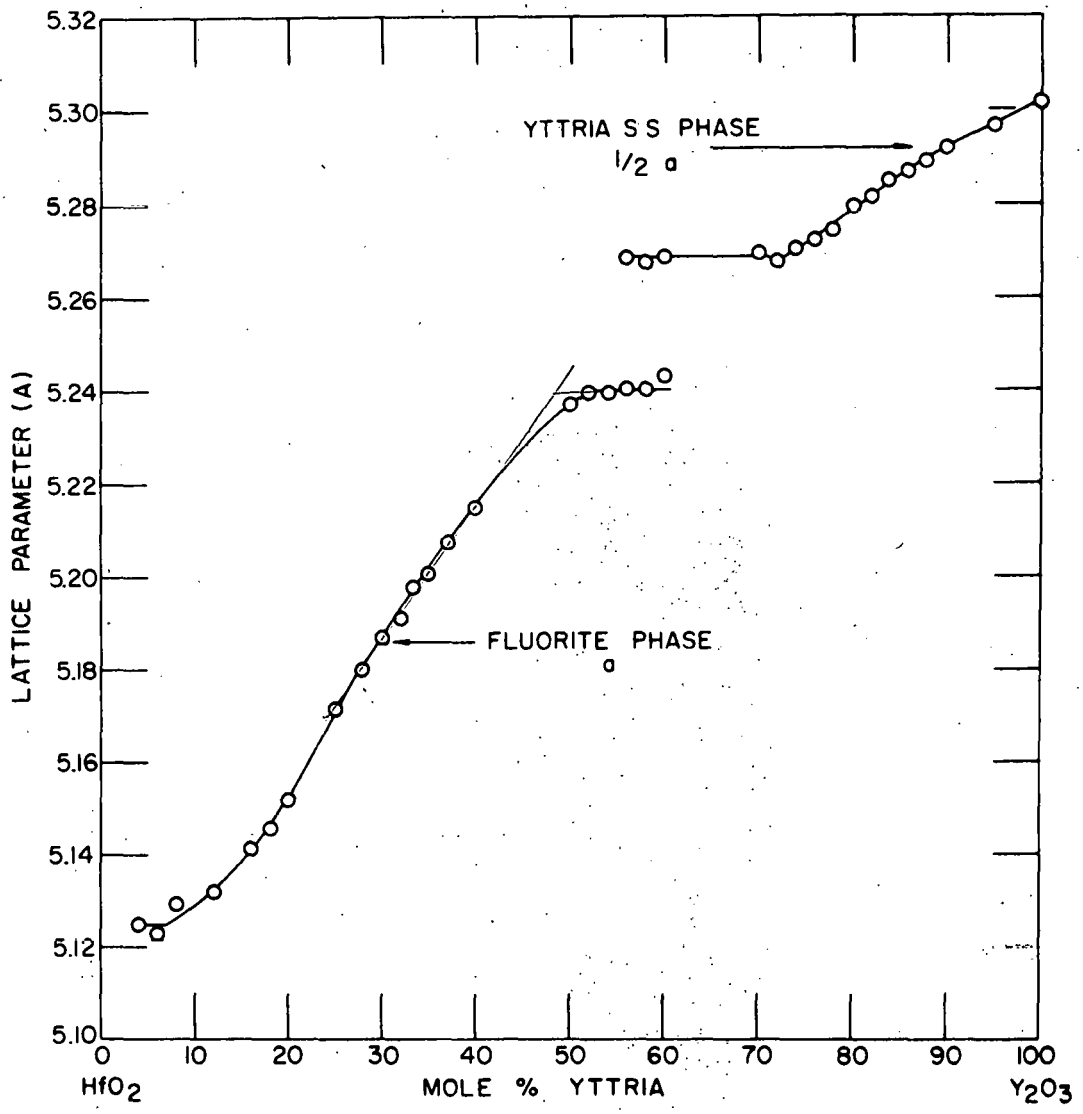


Figure 8. Room temperature lattice parameters of yttria-hafnia compositions cooled from 1600°C

was used to define the boundary as 53 mole % yttria at 1600°C, 54 mole % yttria at 1900°C and 2000°C, and 55 mole % yttria at 2200°C.

No evidence was found in this study of a pyrochlore structure in the yttria-hafnia system. The anomalous increase in the lattice parameter of 33.3 mole % yttria-hafnia reported by Caillet et al. (25) was not observed.

It was difficult to observe the last fluorite peaks present at the upper boundary of the fluorite + yttria solid solution region. As shown in Figure 8 and Appendix A, the change in lattice parameter of the yttria solid solution phase was used to define the boundary. The maximum solubility of hafnia in yttria was found to be about 27 mole % hafnia at 1600° and 2000°C.

The results of the study of phase domains in the yttria-hafnia are summarized in Figure 9. The microstructure in Figure 2 for 70 mole % yttria-hafnia shows two distinct phases. Because of the small grain size of the isolated phase, microprobe analysis was unsuccessful in identifying its composition.

## Liquidus Temperatures

The liquidus temperatures for the yttria-hafnia system are plotted in Figure 9 and tabulated in Appendix B. It is noted that the liquidus temperatures of the fluorite phases remain nearly at the melting point of pure hafnia up to

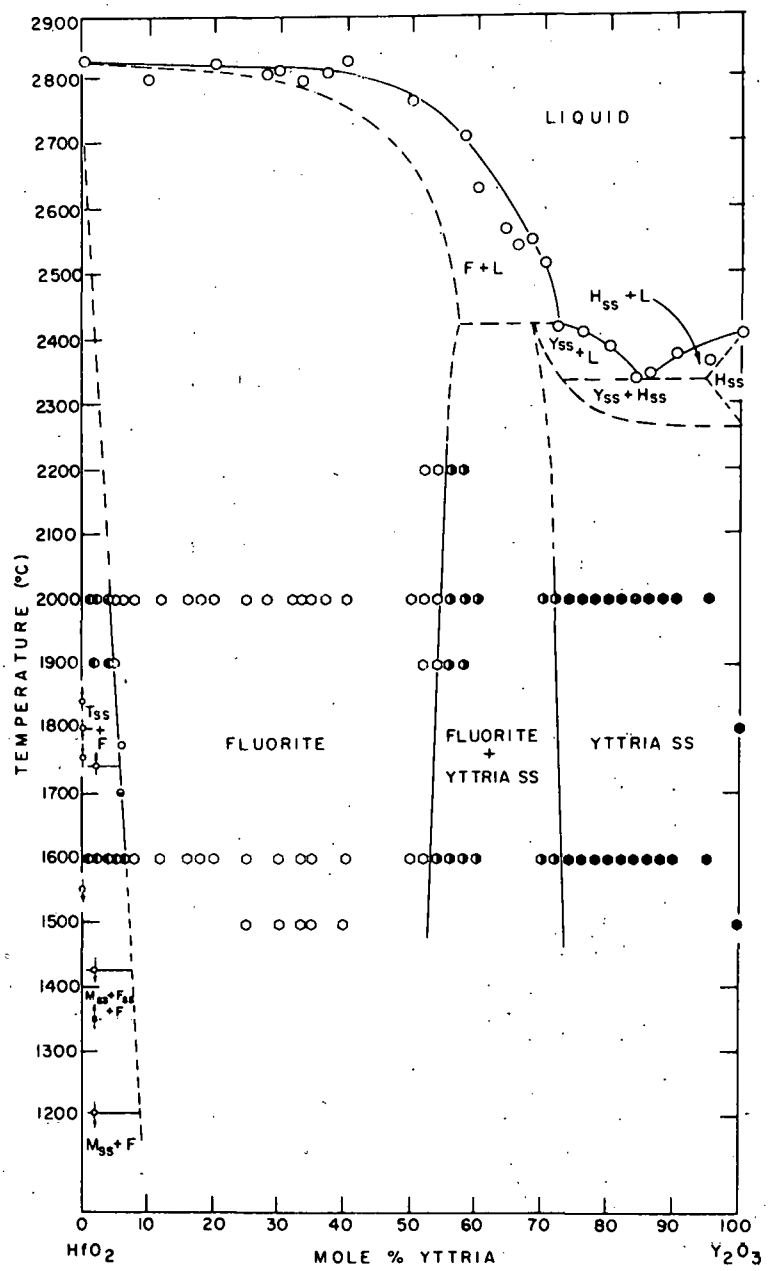


**Figure 9. Tentative phase diagram of the yttria-hafnia system**

compositions containing 40 mole % yttria. Above the composition of 40 mole % yttria, the liquidus drops sharply to a value of 2420°C at 72 mole % yttria. The liquidus continues to drop at a slower rate to the minimum value of 2340°C at 85 mole % yttria. It then increases to 2410°C, the melting point of yttria. With the exception of 3 points, the standard deviation of liquidus temperatures is less than or about equal to 20°C which is the estimated error of temperature measurement with the micro-optical pyrometer at high temperatures (14). The liquidus temperatures of the yttria-rich region of the system agree well with the liquidus found for the zirconia-yttria system by Rouanet (23) using thermal analysis. However, no maximum was observed above the fluorite domain as was reported by Rouanet. Johnstone (14) reports only a slight maximum in the liquidus above the fluorite domain of the erbia-hafnia system.

## Yttria-Hafnia Phase Diagram

The tentative phase diagram of the yttria-hafnia system in Figure 9 incorporates the results of this study with literature data. The lower composition boundary of the fluorite phase was extended to 2700°C to include cubic hafnia found by Boganov *et al.* (13). The hexagonal phase in yttria has been reported by Foex and Traverse (22) and Rouanet (23). The cubic yttria solid solution (Yss) +

hexagonal yttria solid solution (Hss) was taken from Rouanet. However, the solidus curve was modified to allow the peritectic at 2425°C as a means of incorporating the F + Yss two phase domain which appears to extend to the solidus. Rouanet reported no F + Yss two phase domain in the zirconia-yttria system. The eutectic found at 2340°C and 85 mole % yttria is a good agreement with that found by Rouanet at 2380°C at 82.5 mole % yttria.

## Defect Structure of Yttria-Hafnia Fluorite

As yttria is added to hafnia in the fluorite domain, electrical neutrality may be preserved by two defect structures. In the anion vacancy model, the cation sublattice remains filled and neutrality is preserved by the introduction of anion vacancies. Alternately, in the cation interstitial model the anion sublattice remains filled and neutrality is preserved by the introduction of cations on interstitial sites.

Hund (47) has presented a technique to determine which defect structure is present. The measured density is compared to theoretical densities calculated from measured lattice parameters and assumed numbers of atoms per unit cell. Figure 10 and Appendix C give measured apparent density and calculated theoretical densities of yttria-hafnia fluorite compositions. It is easily seen that the anion

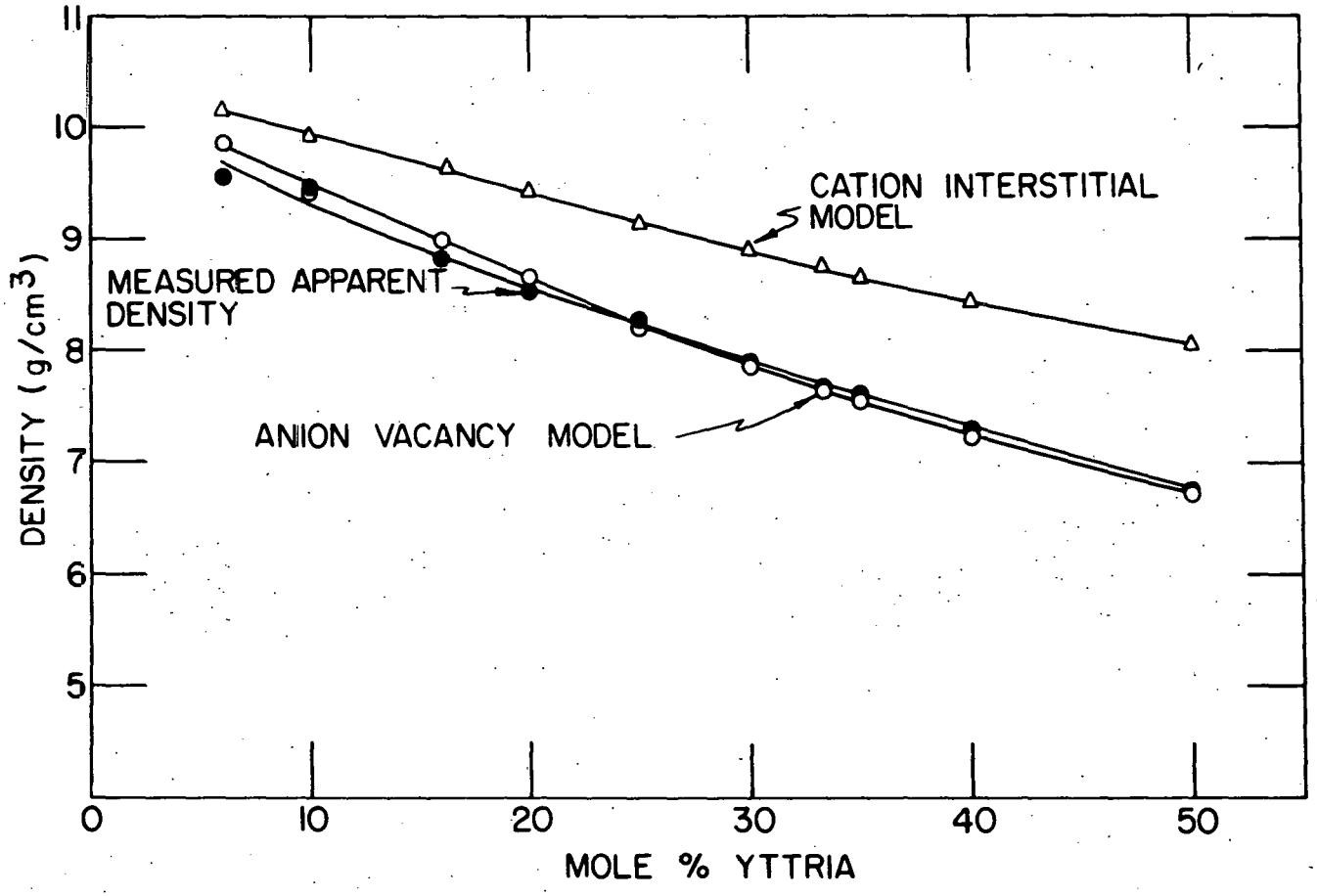


Figure 10. Densities of yttria-hafnia fluorite compositions

vacancy model is appropriate to describe the defect structure of this system.

Compositions from 6 to 20 mole % yttria were sintered at 2000°C for 1 hour and annealed for 30 minutes at 1500°C (3). Compositions of 25 to 50 mole % yttria were annealed at 1600°C for 4 hours. The specimens sintered at 2000°C would be expected to contain a larger percentage of closed pores than ones sintered at 1600°C. This is shown by the measured density curve falling below the anion vacancy model curve at low yttria content.

The anion vacancy defect structure was reported in the zirconia-yttria system by Hund (47), the erbia-hafnia system by Johnstone (14), and in the hafnia rich end of the yttria-hafnia fluorite domain by Schieltz (3).

## Thermal Expansion

### Thoria

Thoria was chosen as a thermal expansion reference because its thermal expansion is well known, it has the same structure as the yttria-hafnia fluorite phase, and it diffracts X-rays well. Figure 11 and Appendix D show the increase in lattice parameter of thoria with increased temperature. The average standard deviation of the high temperature lattice parameters of thoria as computed by the program of Vogel and Kempter (40) is 0.0004 A. The small value of the

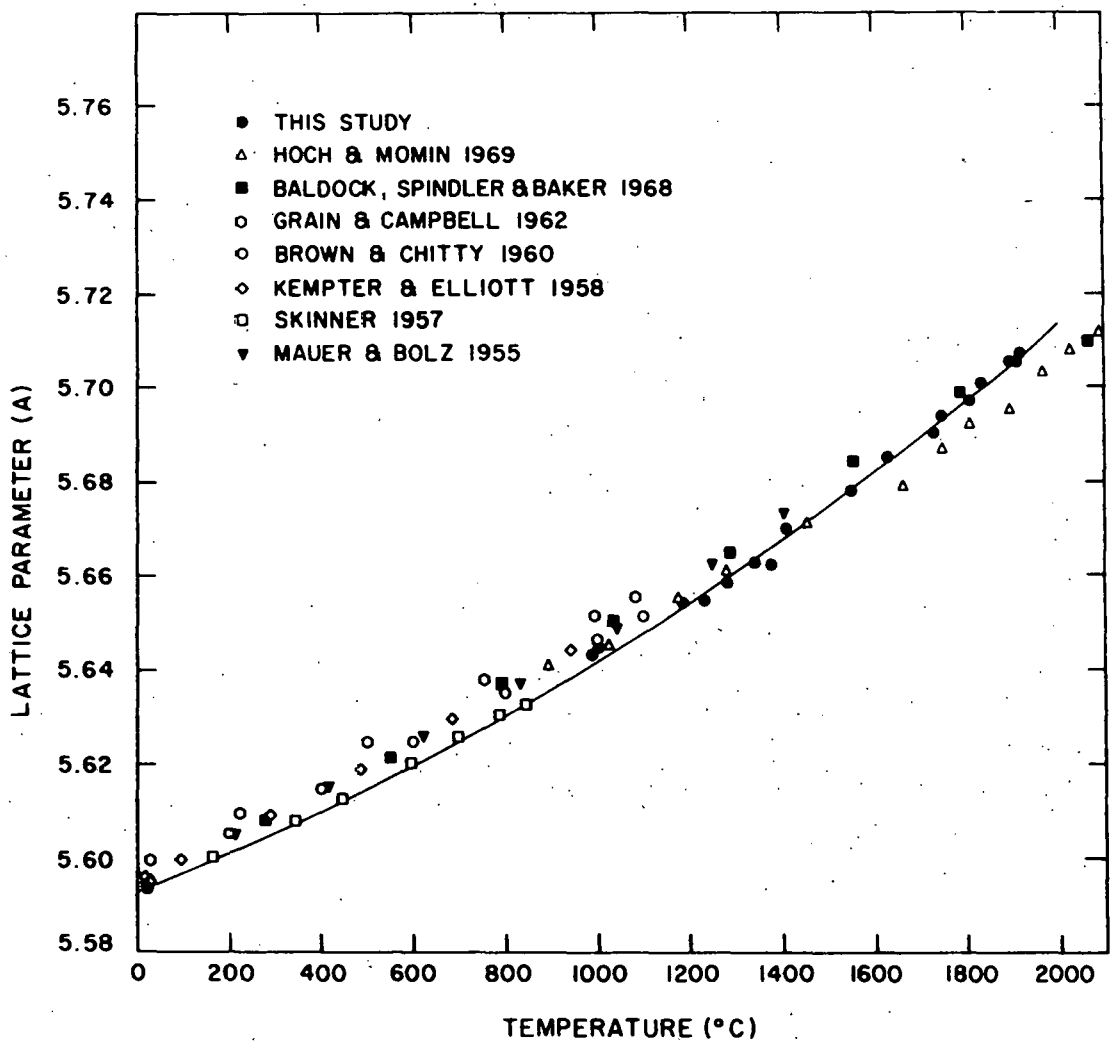


Figure 11. Linear thermal expansion of thoria

standard deviation is indicative of the well defined diffraction patterns obtained at high temperatures. Temperatures were measured with the micro-optical pyrometer and are considered to be accurate within ± 20 $C^{o}$ (14).

The high temperature lattice parameters of thoria are compared with the data of other authors in Figure 11 (48, 49, 50, 51, 52, 53). The percent linear thermal expansion of thoria is presented in Figure 12 and Appendix D. It is compared with the data of other authors in Figure 12 (8, 54, 53, 55). It is seen that the thermal expansion of thoria measured in this study compares well with the results determined by other authors.

A quadratic equation of the form $L = L_o(1+at+bt^2)$ was fitted to the lattice parameter data by nonlinear regression analysis. Yaggee and Foote (56) have found the quadratic expression to be a valid description of the thermal expansion of ceramic materials. The coefficients for the equation and the standard error of estimate (57) are given in Table 8.

Yttria

The increase in the lattice parameter of yttria with temperature is plotted in Figure 13 and tabulated in Appendix E. The average standard deviation of the high temperature lattice parameters as computed by the program of Vogel and Kempter is 0.0015 A. The rather large value of the standard deviation is to be expected because yttrium has a low atomic

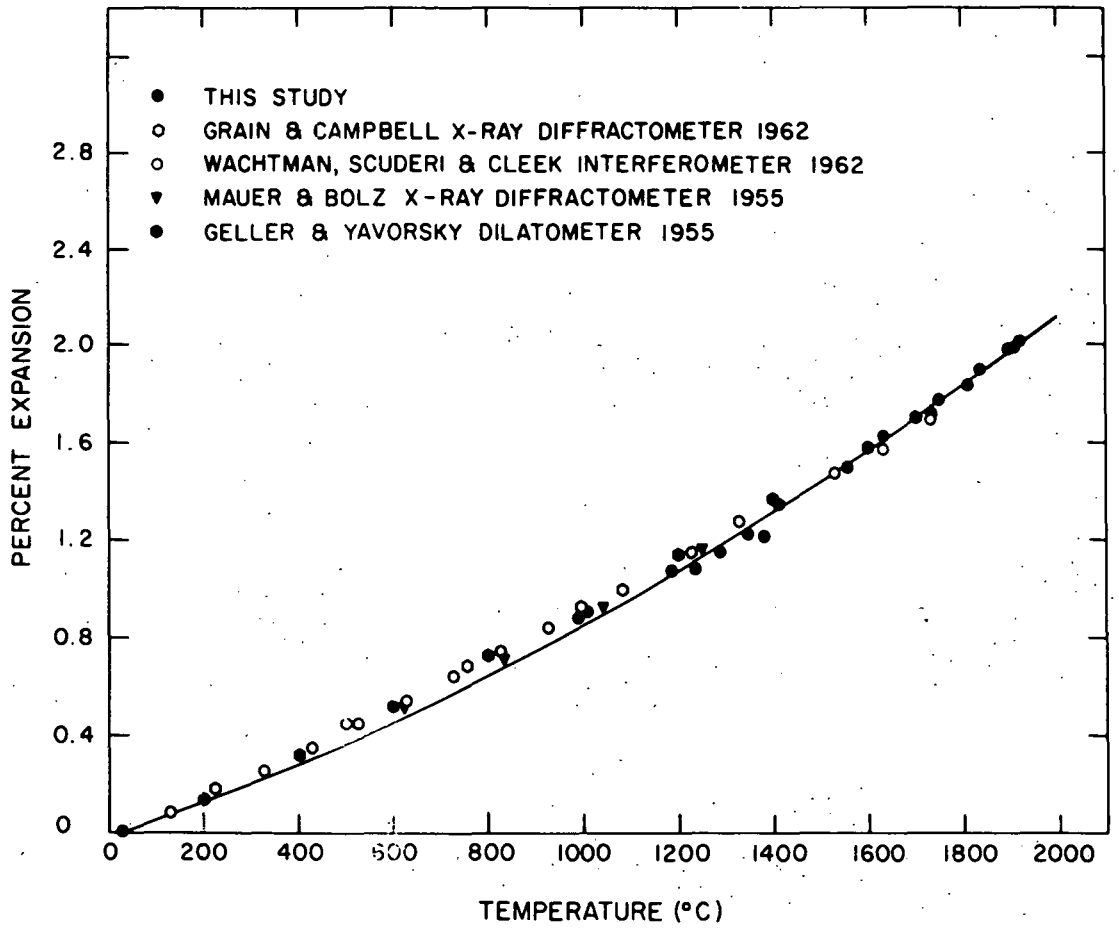


**Figure 12. Percent linear thermal expansion of thoria**

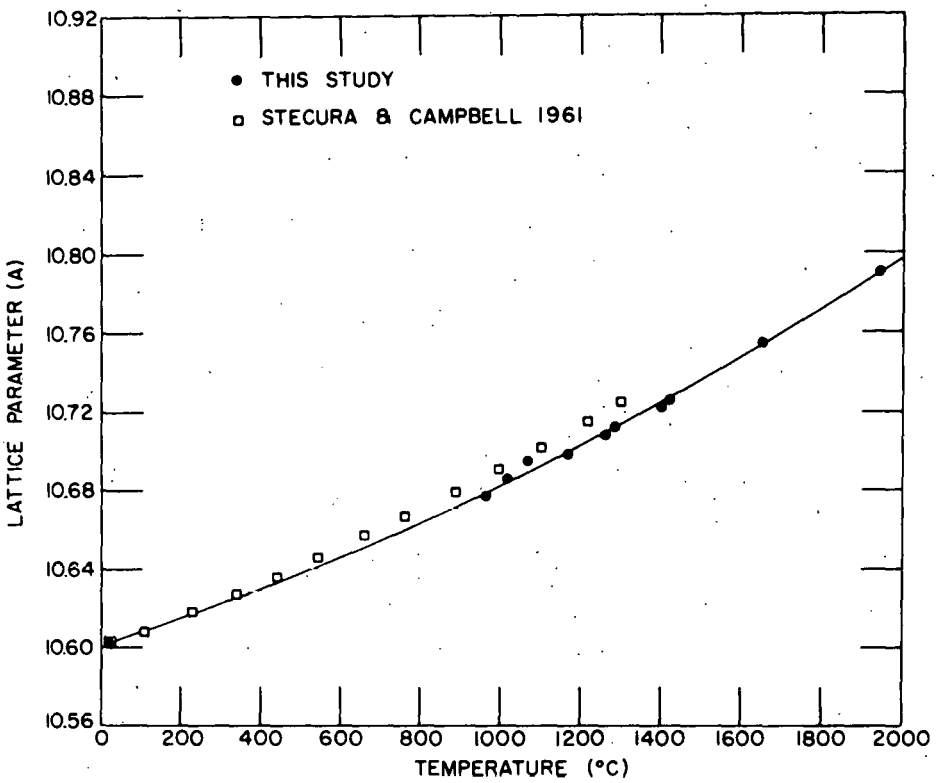


**Figure 13. Linear thermal expansion of yttria**

Table 8. Coefficients of lattice parameter equations $L = L_o(1+at+bt^2)$ where t in °C

| Material | $L_o$ (A) | a x $10^5$ (1/°C) | b x $10^8$ (1/°C) | Standard error of estimate (A) |
|---|---|---|---|---|
| Yttria | 10.6015 | 0.60 | 0.16 | 0.0023 |
| Thoria | 5.5932 | 0.66 | 0.21 | 0.0016 |
| 8 m/o $Y_2O_3$ Fluorite | 5.1196 | 0.61 | 0.26 | 0.0007 |
| 14 " Fluorite | 5.1342 | 0.66 | 0.23 | 0.0019 |
| 20 " Fluorite | 5.1497 | 0.63 | 0.26 | 0.0012 |
| 30 " Fluorite | 5.1832 | 0.71 | 0.19 | 0.0009 |
| 33.3 " Fluorite | 5.1954 | 0.82 | 0.12 | 0.0011 |
| 40 " Fluorite | 5.2143 | 0.74 | 0.15 | 0.0015 |
| 50 " Fluorite | 5.2357 | 0.70 | 0.18 | 0.0014 |

number; therefore yttria does not diffract as well as thoria. The yttria peaks were less intense and more poorly resolved than the thoria peaks.

The lattice parameters determined in this study are lower than those determined by Stecura and Campbell (32). See Figure 13. However, the percent thermal expansion of yttria calculated in this study agree well with the results of Calderwood[1], Stacy (34), and Wilfong et al. (33). See Figure 14.

[1]Calderwood, op. cit.

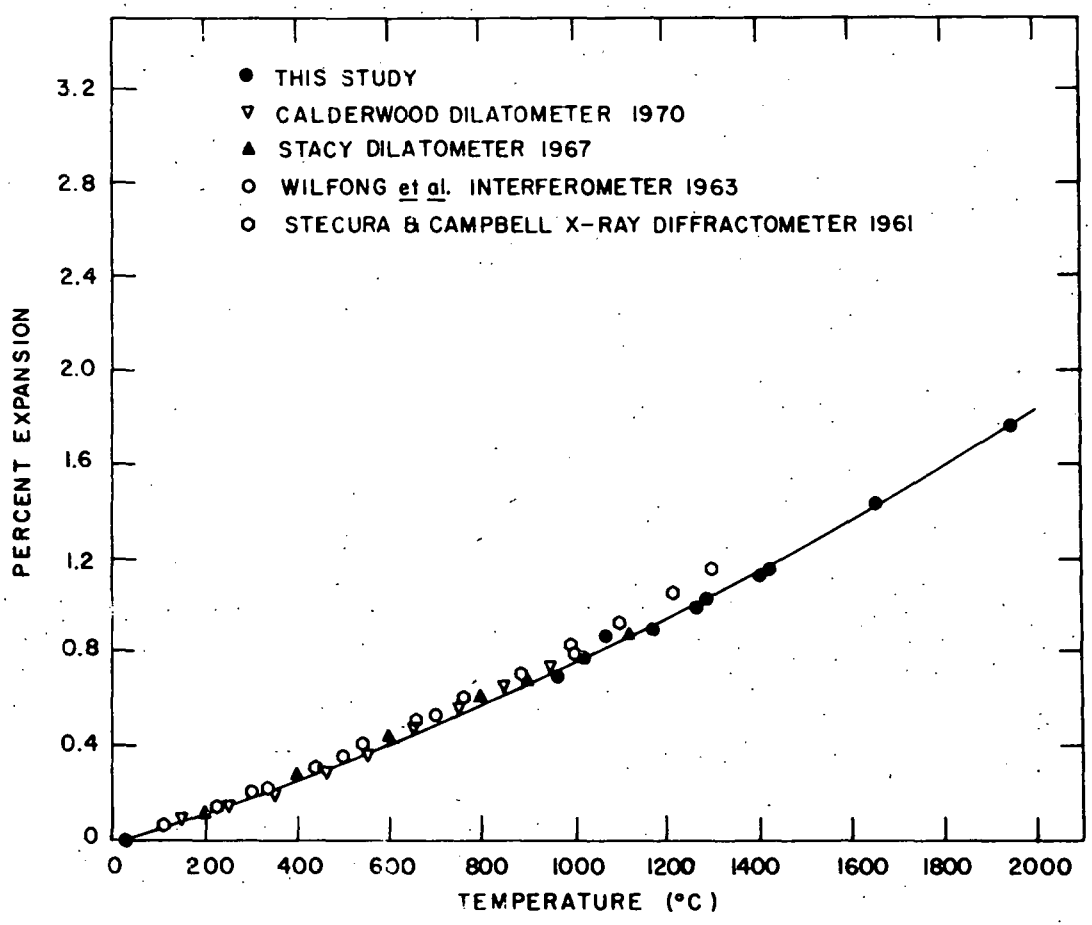


Figure 14. Percent linear thermal expansion of yttria

Coefficients for the quadratic equation of the lattice parameters of yttria and standard error of estimate (57) are presented in Table 8.

Yttria-hafnia fluorite compositions

The thermal expansion of 8, 14, 20, 30, 33.3, 40, and 50 mole % yttria-hafnia fluorite compositions was determined by high temperature X-ray diffraction studies. The increase in lattice parameters as a function of composition and temperature is shown in Figure 15 and tabulated in Appendix F. The average standard deviation of high temperature lattice parameters is 0.0004 A as determined by the method of Vogel and Kempter (40). The temperatures are considered to be accurate to within $\pm 20^{o}C$ (14).

Quadratic equations of the form $L = L_o(1+at+bt^2)$ were fitted to the lattice parameter data by nonlinear regression analysis. The coefficients for the equations and the standard errors of estimate (57) are listed in Table 8. Percent thermal expansion from $25^{o}C$ to several temperatures was computed from the lattice parameter equations and is presented as isotherms in Figure 16. It is noted that at lower temperatures the thermal expansion of 33.3 mole % yttria is a maximum while at higher temperatures the maximum occurs at 20 mole % yttria.

Caillet et al. (25) have observed a maximum at 33.3

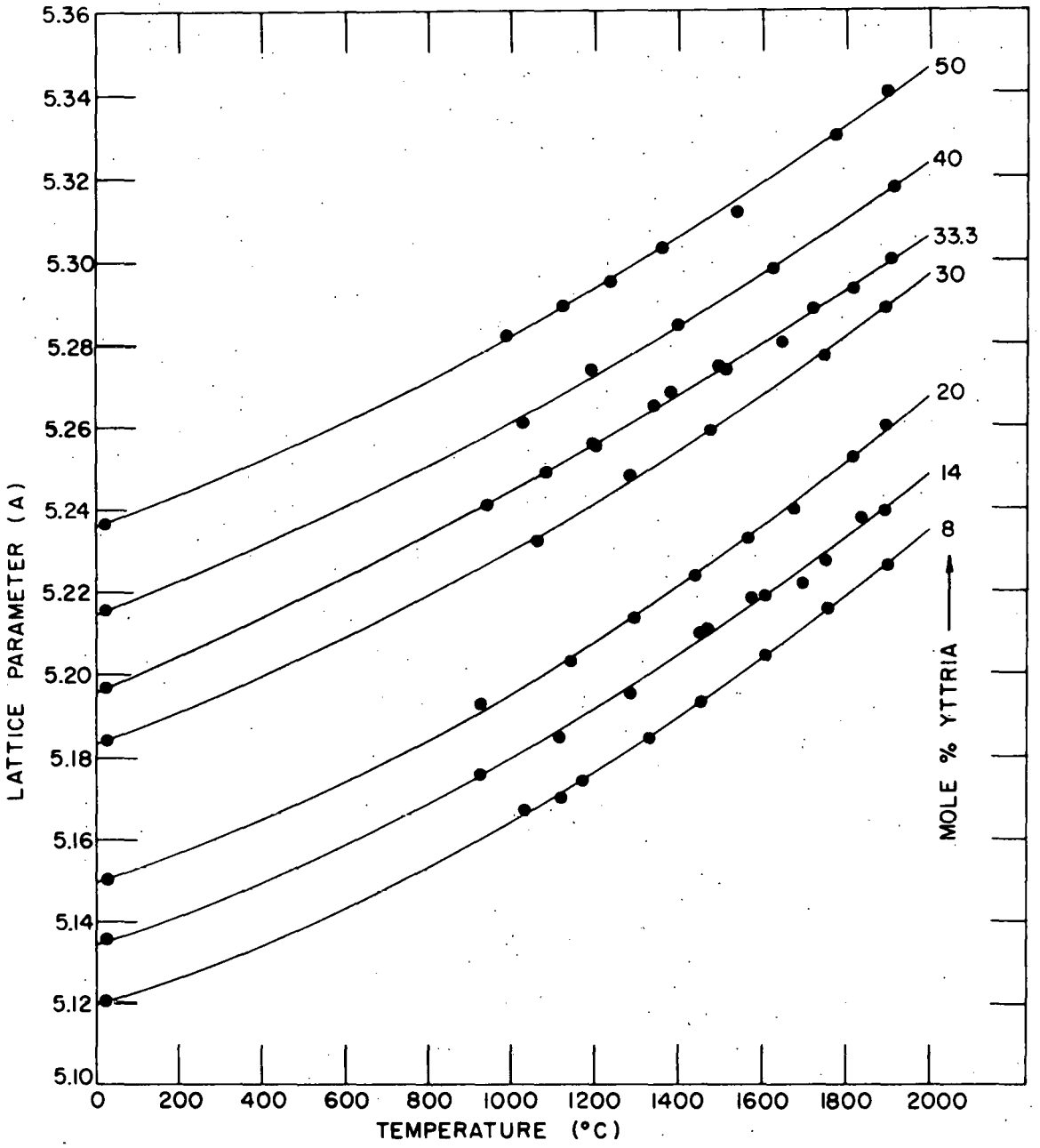


Figure 15. Linear thermal expansion of yttria-hafnia fluorite compositions

Figure 16. Percent linear thermal expansion from 25°C of yttria-hafnia fluorite compositions

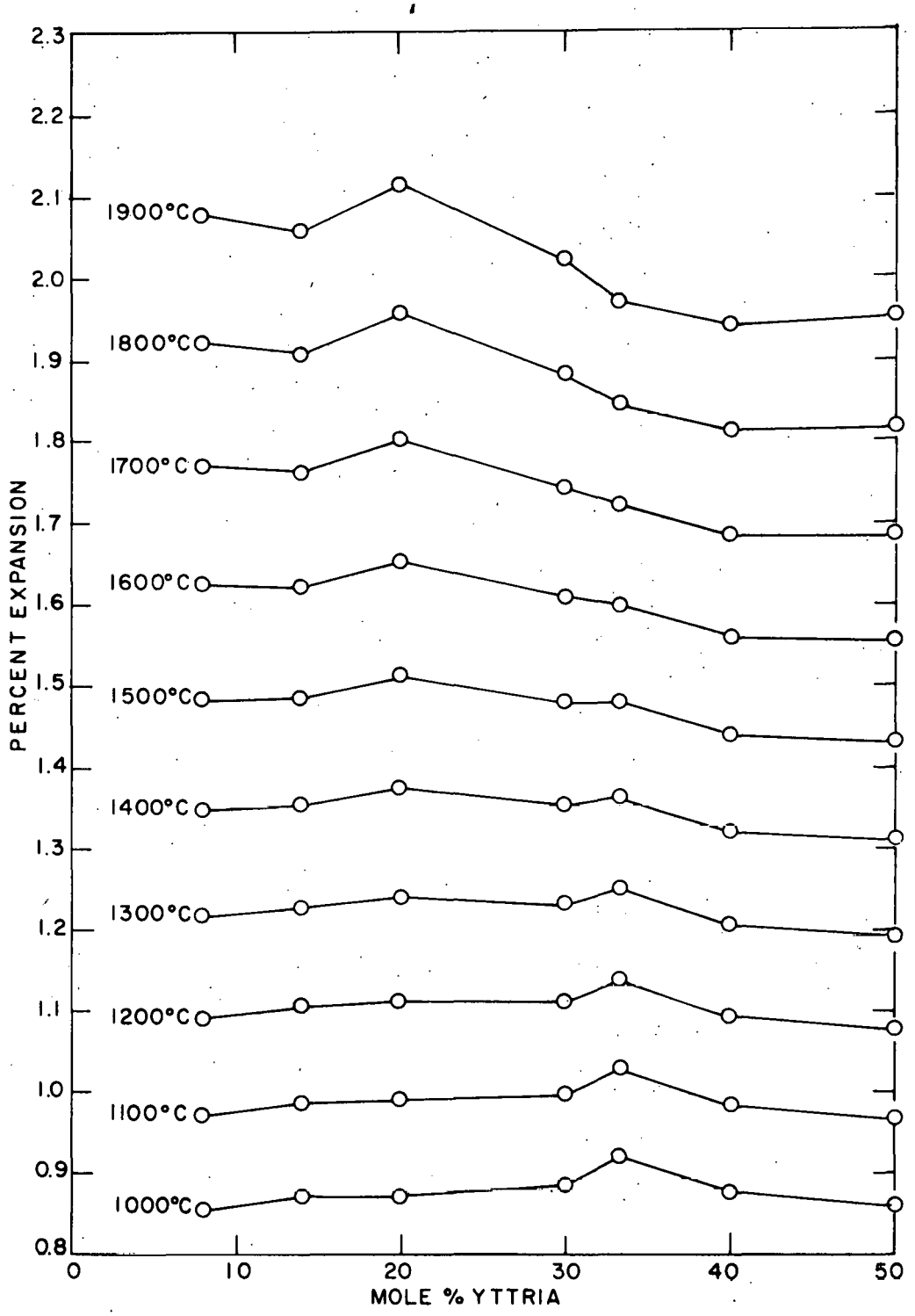
2.3
2.2
2.1
2.0
1.9
1.8
1.7
1.6
1.5
1.4
1.3
1.2
1.1
1.0
0.9
0.8
PERCENT EXPANSION
1900°C
1800°C
1700°C
1600°C
1500°C
1400°C
1300°C
1200°C
1100°C
1000°C
0
10
20
30
40
50
MOLE % YTTRIA

mole % yttria in the thermal expansion coefficient of the yttria-hafnia fluorite compositions calculated in the temperature interval 800° to 1400°C. They interpreted the maximum as being partial evidence for the existence of a pyrochlore phase in the yttria-hafnia system. The thermal expansion coefficients calculated from 800° to 1400°C from equations determined in this study do not show a maximum at 33.3 mole % yttria. The relative maxima seen in Figure 16 are not considered significant.

Thermal expansion data for 8 and 14 mole % yttria-hafnia compositions agree well with those of 8.5 and 12.3 mole % yttria-hafnia studied by Ohnysty and Rose (11).

Monoclinic and tetragonal hafnia

The lattice parameters of monoclinic and tetragonal hafnia as a function of temperature are given in Figure 17 and Appendix G. The average standard deviation of each of the high temperature monoclinic parameters a, b, and c is 0.003 A and $\beta$ is 0.03 degree as computed by the method of Vogel and Kempter (40). The average standard deviation of each of the tetragonal parameters is 0.002 A. No effort was made to fit equations to the lattice parameter data.

It is noted in Figure 17 that monoclinic b remains nearly constant up to 1000°C. It increases slightly to 1400°C and then contracts up to the temperature of the transformation. Monoclinic a and c axes increase over the temper-

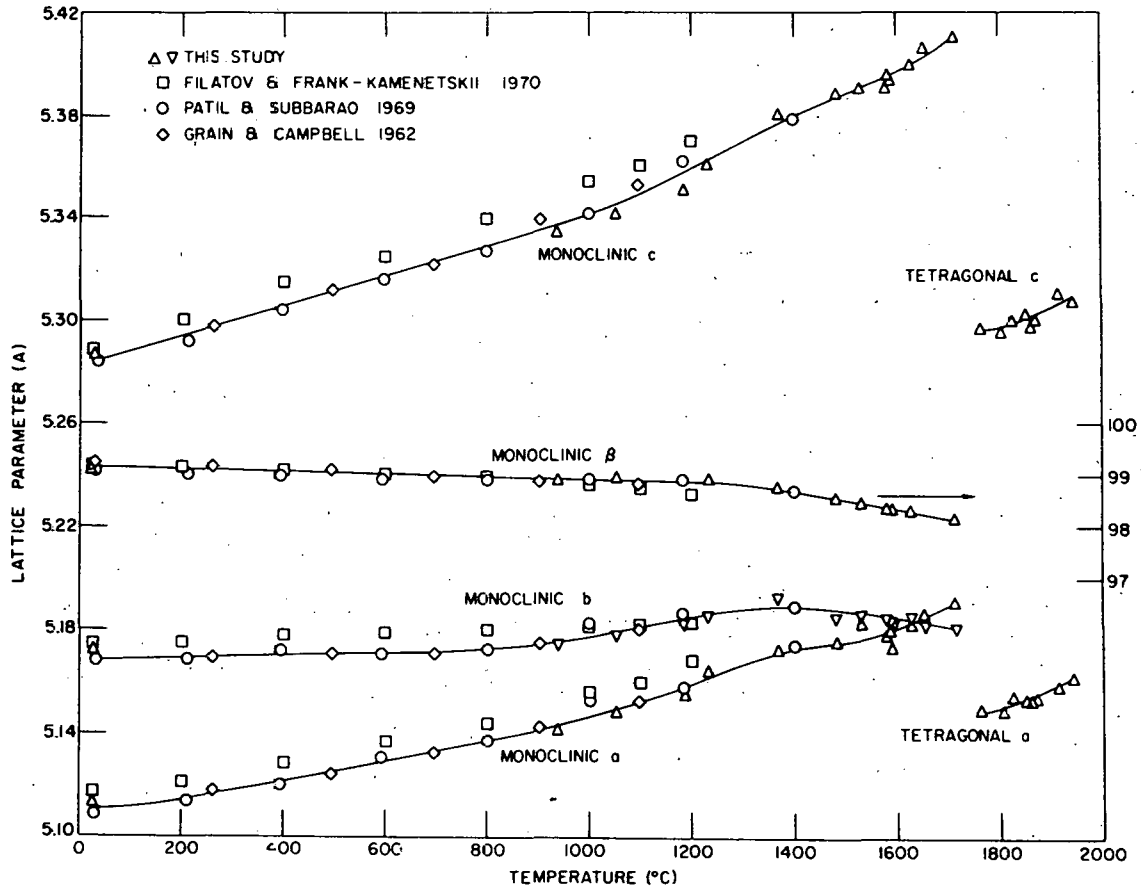


Figure 17. Axial thermal expansion of monoclinic and tetragonal hafnia

ature interval from room temperature to the transformation while $\beta$ decreases slightly. The lattice parameters measured by Filatov and Frank-Kamenetskii (31) are consistently larger than those found by Patil and Subbarao (30), Grain and Campbell (8), or the author. At the temperature of the transformation, the a and b monoclinic parameters are nearly equal. The tetragonal parameters agree well with the high temperature parameters determined by Boganov et al. (13).

The unit cell volumes of monoclinic and tetragonal hafnia are shown in Figure 18 and tabulated in Appendix G. The rapid increase in the unit cell volume at 1400°C is chiefly due to the maximum in the length of the monoclinic b axis. See Figure 17. Based on the values of the monoclinic and tetragonal unit cell volumes at 1750°C, a 2.7% contraction in unit cell volume occurs during the transformation. Similarly, the change in unit cell volume for zirconia during the transformation at 1150°C calculated from the data of Patil and Subbarao (30) was found to be 3.0%.

The percent axial and volume thermal expansions of monoclinic and tetragonal hafnia are plotted in Figure 19 and tabulated in Appendix H. The percent expansions of tetragonal hafnia are based on room temperature values of the corresponding parameter of monoclinic hafnia (30). The thermal expansion of hafnia is shown to be quite anisotropic.

Figure 18. Volume thermal expansion of monoclinic and tetragonal hafnia

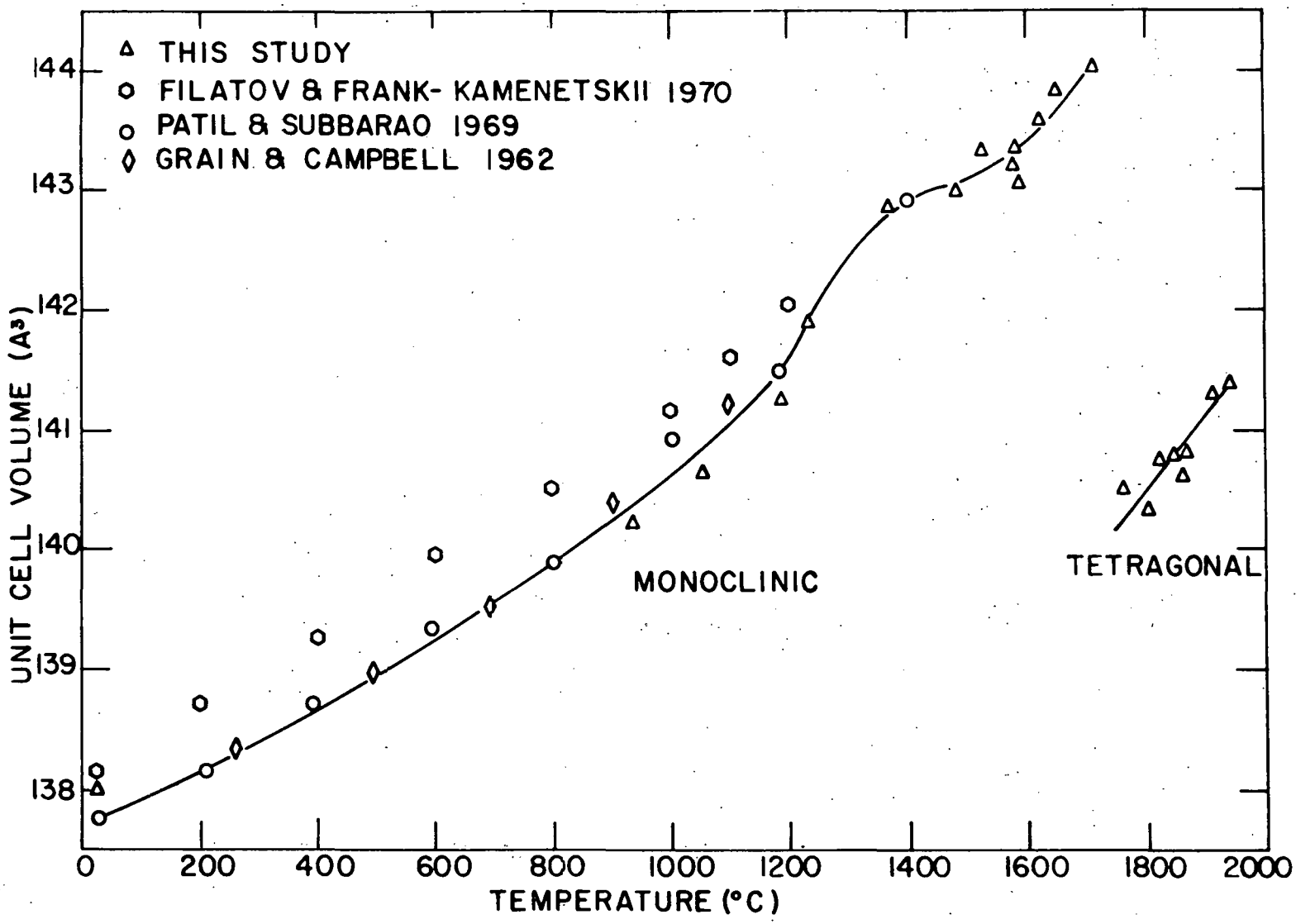
THIS STUDY
FILATOV & FRANK- KAMENETSKII 1970
PATIL & SUBBARAO 1969
GRAIN & CAMPBELL 1962
UNIT CELL VOLUME (A³)
144
143
142
141
140
139
138
0
200
400
600
800
1000
1200
1400
1600
1800
2000
TEMPERATURE (°C)
MONOCLINIC
TETRAGONAL

Figure 19. Percent axial and volume thermal expansions of monoclinic and tetragonal hafnia

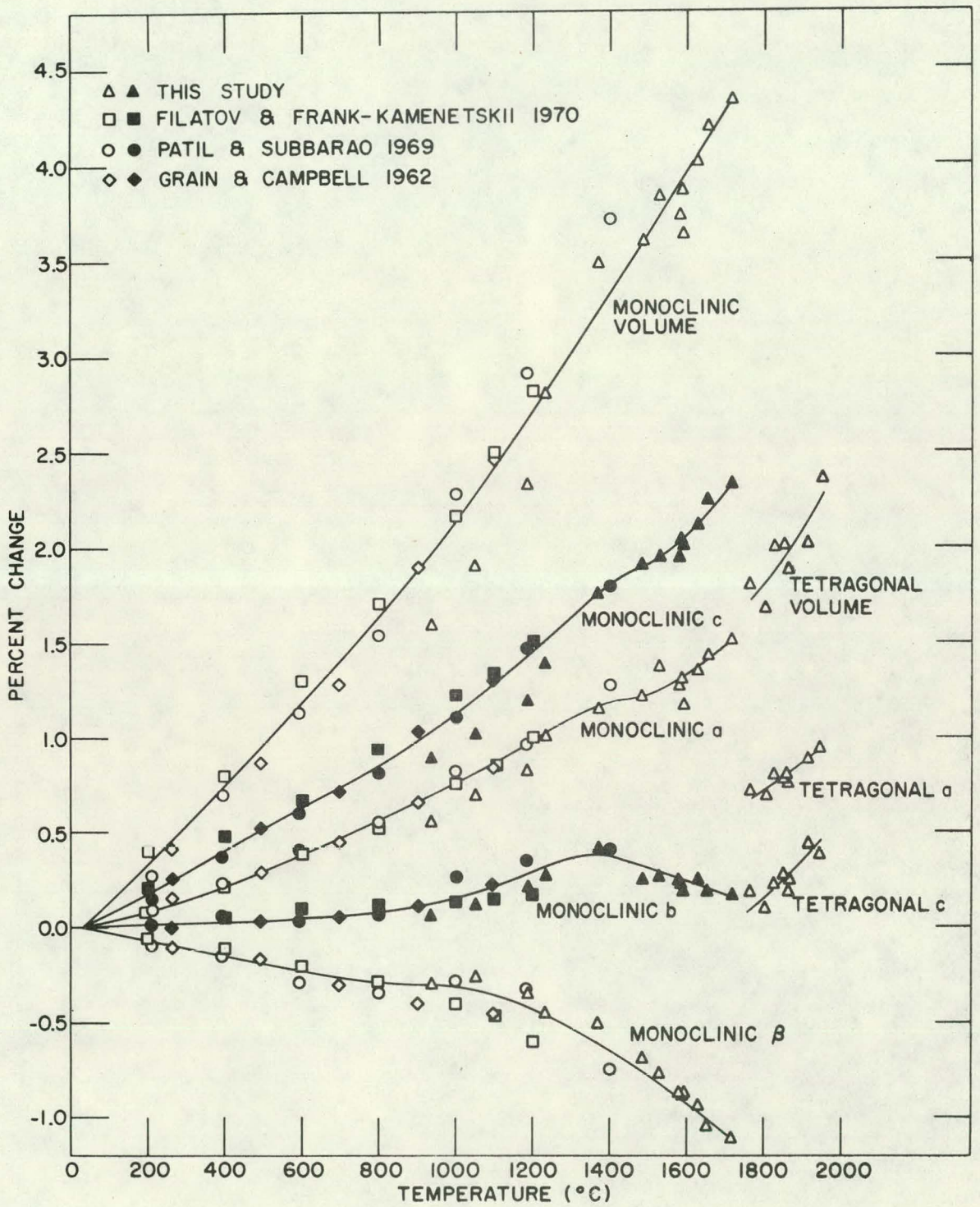
THIS STUDY
FILATOV & FRANK-KAMENETSKII 1970
PATIL & SUBBARAO 1969
GRAIN & CAMPBELL 1962
MONOCLINIC VOLUME
MONOCLINIC c
MONOCLINIC a
MONOCLINIC b
MONOCLINIC β
TETRAGONAL VOLUME
TETRAGONAL a
TETRAGONAL c
PERCENT CHANGE
TEMPERATURE (°C)
4.5
4.0
3.5
3.0
2.5
2.0
1.5
1.0
0.5
0.0
-0.5
-1.0
0
200
400
600
800
1000
1200
1400
1600
1800
2000

# CONCLUSIONS

1. The monoclinic-to-tetragonal phase transformation of hafnia was found to start at 1750°C and end at 1850°C on heating. The reverse transformation on cooling began at 1800°C and was complete at 1550°C.

2. The decrease in the unit cell volume of hafnia during the monoclinic-to-tetragonal phase transformation was found to be 2.7 % at 1750°C.

3. Below 2000°C, the solubility of yttria in hafnia is less than 1 mole %. This slight solubility causes the monoclinic-to-tetragonal transformation to occur at much lower temperatures than in pure hafnia.

4. In the yttria-hafnia system, a two phase domain of hafnia solid solution and stabilized fluorite phase extends from less than 1 mole % yttria to 7 mole % yttria at 1600°C and to 4 mole % yttria at 2000°C. The single fluorite domain then extends to 53 mole % yttria at 1600°C and to 55 mole % yttria at 2200°C.

5. Yttria shows a large solubility for hafnia. The single phase yttria solid solution domain extends from pure yttria to about 73 mole % yttria at 1600° and 2000°C. The yttria solid solution domain is separated from the fluorite domain by a two phase region which appears to extend to the solidus.

6. The liquidus curve for the yttria-hafnia system

remains nearly at the melting point of hafnia up to 40 mole % yttria. Beyond 40 mole % yttria, the liquidus drops sharply to 2425°C at 72 mole % yttria. It decreases at a slower rate to the minimum of 2340°C at 85 mole % yttria and then increases to 2410°C, the melting point of yttria.

7. As yttrium substitutes for hafnium in the yttria-hafnia fluorite phase, the charge neutrality is preserved by the formation of an anion vacancy defect structure.

8. The mean thermal expansion coefficients from 25° to 2000°C for the yttria-hafnia fluorite phases are about $1.1 \times 10^{-5}$ in./in.°C. The mean thermal expansion coefficient for yttria over the same temperature interval was found to be $9.3 \times 10^{-6}$ in./in.°C.

9. A stable high temperature ceramic material may be produced by adding from 10 to 50 mole % yttria to hafnia. The thermal expansion coefficient and liquidus temperature vary only slightly over this range of composition.

# BIBLIOGRAPHY


1. Buckley, J. D. and Wilder, D. R. Effects of cyclic heating and thermal shock on hafnia stabilized with calcia, magnesia, and yttria. NASA TN (Technical Note) D-5279 [National Aeronautics and Space Administration, Washington, D.C.]. 1969.

2. Ezerskii, M. L., Kolesnikov, E. I., Shklyarevskii, E. E., and Rastorguev, L. N. Some properties of atomized layers of stabilized zirconium dioxide. Inorganic Materials 4: 1398-1400. 1968.

3. Schieltz, J. D. Electrolytic behavior of yttria and yttria stabilized hafnia. Unpublished Ph.D. thesis. Ames, Iowa, Library, Iowa State University of Science and Technology. 1970.

4. Adam, J. and Rogers, M. D. The crystal structure of $ZrO_2$ and $HfO_2$. Acta Crystallographica 12: 951. 1959.

5. Ruh, R. and Corfield, P. W. R. Crystal structure of monoclinic hafnia and comparison with monoclinic zirconia. American Ceramic Society Journal 53: 126-129. 1970.

6. Ruh, R., Garrett, H. J., Domagala, R. F., and Tallan, N. M. The system zirconia-hafnia. American Ceramic Society Journal 51: 23-27. 1968.

7. Wolten, G. M. Diffusionless phase transformations in zirconia and hafnia. American Ceramic Society Journal 46: 418-422. 1963.

8. Grain, C. F. and Campbell, W. J. Thermal expansion and phase inversion of six refractory oxides. U.S. Bureau of Mines Report of Investigations 5982. 1962.

9. Baun, W. L. Phase transformations at high temperatures in hafnia and zirconia. Science 140: 1330-1331. 1963.

10. Curtis, C. E., Doney, L. M., and Johnson, J. R. Some properties of hafnium oxide, hafnium silicate, calcium hafnate, and hafnium carbide. American Ceramic Society Journal 37: 458-465. 1954.

11. Ohnysty, B. and Rose, F. K. Thermal expansion measurements on thoria and hafnia to 4500°F. American Ceramic Society Journal 47: 398-400. 1964.

12. Stansfield, O. M. Thermal expansion of polycrystalline $HfO_2$-$ZrO_2$ solid solutions. American Ceramic Society Journal 48: 436-437. 1965.

13. Boganov, A. G., Rudenko, V. S., and Makarov, L. P. X-ray investigation of zirconium and hafnium oxides at temperatures up to 2750°. Academy of Sciences of the U.S.S.R. Proceedings Chemistry Section 160: 146-148. 1965.

14. Johnstone, J. K. The erbia-hafnia system. Unpublished Ph.D. thesis. Ames, Iowa, Library, Iowa State University of Science and Technology. 1970.

15. Isupova, E. N., Glushkova, V. B., and Keler, E. K. The $Y_2O_3$-$HfO_2$ system in the region rich in hafnium dioxide. Inorganic Materials 5: 1658-1661. 1969.

16. Smith, D. K. and Newkirk, H. W. The crystal structure of badeleyite (monoclinic $ZrO_2$) and its relation to the polymorphism of $ZrO_2$. Acta Crystallographica 18: 983-991. 1965.

17. Teufer, G. Crystal structure of tetragonal $ZrO_2$. Acta Crystallographica 15: 1187. 1962.

18. Smith, D. K. and Cline, C. F. Verification of existence of cubic zirconia at high temperature. American Ceramic Society Journal 45: 249-250. 1962.

19. Engelke, J. L., Halden, F. A., and Farley, E. P. Synthesis of new high temperature materials. U.S. Atomic Energy Commission Report WADC-TR-59-654 [Wright Air Development Center, Wright-Patterson AFB, Ohio] . 1960.

20. Swanson, H. E., Fuyat, R. H., and Ugrinic, G. M. Standard X-ray diffraction powder patterns. National Bureau of Standards Circular 539. Vol. 3. 1954.

21. Henry, N. F. M. and Lonsdale, K., eds. International tables for X-ray crystallography. Vol. 1. Birmingham, England, Kynoch Press. 1952.

22. Foex, M. and Traverse, J. Etude a haute temperature des transformations allotropiques des sesquioxydes d'yttrium, d'erbium, et de thulium. Academie des Sciences Comptes Rendus, Serie C, 267: 2490-2493. 1965.

23. Rouanet, A. Diagrammes de solidification et diagrammes de phases de haute temperature des systemes zircone-oxyde d'erbium, zircone-oxyde d'yttrium, et zircone-oxyde d'ytterbium. Academie des Sciences Comptes Rendus, Serie C, 267: 1581-1584. 1968.

24. Besson, J., Deportes, C., and Robert, G. Conductibilite electrique dans le systeme oxyde de hafnium-oxyde d' yttrium a haute temperature. Academie des Sciences Comptes Rendus, Serie C, 262: 527-530. 1966.

25. Caillet, M., Deportes, C., Robert, G., and Vitter, G. Etude structurale dans le systeme $HfO_2$-$Y_2O_3$. Revue International des Hautes Temperatures et des Refractaires 4: 269-271. 1967.

26. Roth, R. S. Pyrochlore-type compounds containing double oxides of trivalent and tetravalent ions. National Bureau of Standards Journal of Research 56: 17-25. 1956.

27. Perez y Jorba, M. Contribution a l'etude des systemes zircone-oxydes de terres rares. Annales de Chimie 7: 479-511. 1962.

28. Komissarova, L. N., Ken-Shih, W., and Spitsyn, V. I. Reaction of hafnium hydroxide with the hydroxides of yttrium, lanthanum, neodymium, and ytterbium. Inorganic and Analytical Chemistry, No. 1: 1-7. 1963.

29. Smith, D. K. The nonexistence of yttrium zirconate. American Ceramic Society Journal 49: 625-626. 1966.

30. Patil, R. N. and Subbarao, E. C. Axial thermal expansion of $ZrO_2$ and $HfO_2$ in the range room temperature to 1400°C. Journal of Applied Crystallography 2: 281-288. 1969.

31. Filatov, S. K. and Frank-Kamenetskii, V. A. Anomalous thermal expansion of $ZrO_2$ and $HfO_2$ over the range 20-1200°C. Soviet Physics-Crystallography 14: 696-699. 1970.

32. Stecura, S. and Campbell, W. J. Thermal expansion and phase inversions of rare-earth oxides. U.S. Bureau of Mines Report of Investigations 5847. 1961.

33. Wilfong, R. L., Domingues, L. P., Furlong, L. R., and Finlayson, J. A. Thermal expansion of the oxides of yttrium, cerium, samarium, europium, and dysprosium. U.S. Bureau of Mines Report of Investigations 6180. 1963.

34. Stacy, D. W. Thermal expansion of the sesquioxides of yttrium, scandium, and gadolinium. Unpublished M.S. thesis. Ames, Iowa, Library, Iowa State University of Science and Technology. 1967.

35. Lynch, C. T. Hafnium oxide. In Alper, A. M., ed. High temperature oxides part 2. Oxides of rare earths, titanium, zirconium, hafnium, niobium, and tantalum. New York, New York, Academic Press. 1970.

36. Vivien, D., Livage, J., and Mazieres, C. Nature of the precipitated hydrated oxides of the elements of group IV A. I Thermal analysis and infrared spectroscopy. Journal de Chimie Physique et de Physico-Chimie Biologique 67: 199-204. 1970.

37. Berard, M. F., Wirkus, C. D., and Wilder, D. R. Diffusion of oxygen in selected monocrystalline rare earth oxides. American Ceramic Society Journal 51: 643-647. 1968.

38. Dvorak, J. R. and Domagala, R. F. Metallographic processing of oxide specimens. U.S. Atomic Energy Commission Report CONF-670533 [21st AEC Metallographic Group Meeting, Upton, New York. May 10-12, 1967]. 1967.

39. Andrews, A. I. Ceramic tests and calculations. New York, New York, John Wiley and Sons, Inc. 1928.

40. Vogel, R. E. and Kempter, C. P. A mathematical technique for the precision determination of lattice parameters. Acta Crystallographica 14: 1130-1134. 1961.

41. Cullity, B. D. Elements of X-ray diffraction. Reading, Massachusetts, Addison-Wesley Publishing Company, Inc. 1956.

42. Wood, W. P. and Cork, J. M. Pyrometry. New York, New York, McGraw-Hill Book Company, Inc. 1941.

43. Stimson, J. F. International practical temperature scale of 1948. Text revision of 1960. National Bureau of Standards Journal of Research, Section A, 65: 139-145. 1961.

44. Gubareff, G. G., Janssen, J. E., and Torborg, R. H. Thermal radiation properties survey. 2nd ed. Minneapolis, Minnesota, Honeywell Research Center. 1960.

45. Schneider, S. J. Compilation of the melting points of the metal oxides. U.S. National Bureau of Standards Monograph 68. 1963.

46. Duwez, P., Brown, F. H., Jr., and Odell, F. The zirconia-yttria system. Electrochemical Society Journal 98: 356-362. 1951.

47. Hund, F. Anomalous mixed crystals in the system $ZrO_2$-$Y_2O_3$. Zeitschrift fuer Electrochemie 55: 363-366. 1951.

48. Hoch, M. and Momin, A. C. High temperature thermal expansion of $UO_2$ and $ThO_2$. High Temperatures - High Pressures. International Journal of Research 1: 401-407. 1969.

49. Baldock, P. J., Spindler, W. E., and Baker, T. W. An X-ray study of the variation of the lattice parameters of alumina, magnesia, and thoria up to 2000°C. United Kingdom Atomic Energy Authority AERE-R-5674 [Atomic Energy Research Establishment, Harwell, Berks, England]. 1968.

50. Brown, A. and Chitty, A. Thoria as a fertile component for a liquid metal breeder blanket. Journal of Nuclear Energy, Part B: Reactor Technology 1: 145-152. 1960.

51. Kempter, C. P. and Elliott, R. O. Thermal expansion of <UN>, <$UO_2$>, <$UO_2 \cdot ThO_2$>, and <$ThO_2$>. The Journal of Chemical Physics 30: 1524-1526. 1959.

52. Skinner, B. J. The thermal expansions of thoria, periclase, and diamond. The American Mineralogist 42: 39-55. 1957.

53. Mauer, F. A. and Bolz, L. H. Measurement of thermal expansion of cermet components by high temperature X-ray diffraction. U.S. Atomic Energy Commission Report WADC-TR-55-473 [Wright Air Development Center, Wright-Patterson AFB, Ohio]. 1955.

54. Wachtman, J. B., Jr., Scuderi, T. G., and Cleek, G. W. Linear thermal expansion of aluminim oxide and thorium oxide from 100° to 1100°K. American Ceramic Society Journal 45: 319-323. 1962.

55. Geller, R. F. and Yavorsky, P. J. Effects of some oxide additions on the thermal length changes of zirconia. U.S. National Bureau of Standards Journal of Research 35: 87-110. 1945.

56. Yaggee, F. L. and Foote, F. G. A method for reconstructing a thermal expansion graph from two values of the mean expansion coefficient. U.S. Atomic Energy Commission Report ANL-7644 [Argonne National Laboratory, Argonne, Illinois]. 1969.

57. Crow, E. L., Davis, F. A., and Maxfield, M. W. Statistics manual. New York, New York, Dover Publications, Inc. 1960.

# APPENDICES

**Appendix A. Room temperature lattice parameters of yttria-hafnia compositions cooled from 1600°C.**

| Composition (mole % yttria) | Lattice parameter (A) Fluorite | Yttria solid solution |
|---|---|---|
| 4 | 5.1249[a] | |
| 6 | 5.1230 | |
| 8 | 5.1290 | |
| 12 | 5.1317 | |
| 16 | 5.1413 | |
| 18 | 5.1455 | |
| 20 | 5.1518 | |
| 25 | 5.1717 | |
| 28 | 5.1797 | |
| 30 | 5.1869 | |
| 32 | 5.1910 | |
| 33.3 | 5.1976 | |
| 35 | 5.2007 | |
| 37 | 5.2074 | |
| 40 | 5.2146 | |
| 50 | 5.2368 | |
| 52 | 5.2394 | |
| 54 | 5.2394 | |
| 56 | 5.2402 | 10.536[b] |
| 58 | 5.2401 | 10.535 |
| 60 | 5.2434 | 10.537 |
| 70 | | 10.539 |
| 72 | | 10.535 |
| 74 | | 10.541 |
| 76 | | 10.544 |
| 78 | | 10.548 |
| 80 | | 10.559 |
| 82 | | 10.562 |
| 84 | | 10.570 |
| 86 | | 10.573 |
| 88 | | 10.578 |
| 90 | | 10.583 |
| 95 | | 10.593 |
| 100 | | 10.603 |

[a]Average standard deviation of fluorite lattice parameters as determined by the program of Vogel and Kempter (40) is 0.0003 A.

[b]Average standard deviation of yttria solid solution lattice parameters is 0.001 A.

**Appendix B. Liquidus temperatures of yttria-hafnia compositions**

| Composition (mole % yttria) | Liquidus temperature | Number of determinations | Standard deviation |
|---|---|---|---|
| 0 | 2825 | 10 | 11 |
| 10 | 2796 | 4 | 4 |
| 20 | 2820 | 3 | 3 |
| 28 | 2804 | 2 | 4 |
| 30 | 2811 | 4 | 19 |
| 33.3 | 2794 | 3 | 12 |
| 37 | 2803 | 2 | 10 |
| 40 | 2825 | 3 | 11 |
| 50 | 2764 | 6 | 15 |
| 58 | 2708 | 3 | 9 |
| 60 | 2630 | 6 | 16 |
| 64 | 2568 | 2 | 21 |
| 66 | 2544 | 3 | 53 |
| 68 | 2551 | 3 | 6 |
| 70 | 2516 | 4 | 43 |
| 72 | 2420 | 3 | 3 |
| 76 | 2411 | 5 | 34 |
| 80 | 2389 | 6 | 14 |
| 84 | 2341 | 3 | 7 |
| 86 | 2348 | 3 | 12 |
| 90 | 2380 | 9 | 21 |
| 95 | 2368 | 5 | 6 |
| 100 | 2410 | 10 | 5 |

## Appendix C. Densities of yttria-hafnia fluorite compositions

| Composition (mole % yttria) | Theoretical density Vacancy[a] model ($gm/cm^3$) | Theoretical density Interstitial[b] model ($gm/cm^3$) | Measured apparent density ($gm/cm^3$) |
|---|---|---|---|
| 6 | 9.859 | 10.146 | 9.566 |
| 10 | 9.490 | 9.941 | 9.437 |
| 16 | 8.979 | 9.644 | 8.832 |
| 20 | 8.654 | 9.441 | 8.524 |
| 25 | 8.232 | 9.147 | 8.280 |
| 30 | 7.874 | 8.901 | 7.893 |
| 33.3 | 7.664 | 8.759 | 7.685 |
| 35 | 7.552 | 8.677 | 7.605 |
| 40 | 7.247 | 8.455 | 7.322 |
| 50 | 6.725 | 8.070 | 6.749 |

[a] Vacancy model:

$$\rho = \frac{4\ (x\ (\text{mol. wt. } Y_2O_3) + (1-x)(\text{mol. wt. } HfO_2))}{0.6023\ (x+1)\ a_o^3}$$

[b] Interstitial model:

$$\rho = \frac{4\ (x\ (\text{mol. wt. } Y_2O_3) + (1-x)(\text{mol. wt. } HfO_2))}{0.6023\ (1 + x/2)\ a_o^3}$$

x = mole fraction Yttria.

$a_o$ = lattice parameter.

## Appendix D. Linear thermal expansion of thoria

| Temperature (°C) | Lattice parameter (A) | Percent linear expansion (%) |
|---|---|---|
| 25 | 5.5939 | 0.000 |
| 990 | 5.6432 | 0.881 |
| 1009 | 5.6448 | 0.910 |
| 1187 | 5.6543 | 1.080 |
| 1235 | 5.6545 | 1.083 |
| 1285 | 5.6585 | 1.155 |
| 1345 | 5.6626 | 1.228 |
| 1379 | 5.6622 | 1.221 |
| 1410 | 5.6698 | 1.357 |
| 1555 | 5.6779 | 1.502 |
| 1630 | 5.6851 | 1.630 |
| 1733 | 5.6902 | 1.722 |
| 1749 | 5.6939 | 1.788 |
| 1810 | 5.6970 | 1.843 |
| 1836 | 5.7008 | 1.911 |
| 1896 | 5.7054 | 1.993 |
| 1907 | 5.7056 | 1.997 |
| 1918 | 5.7072 | 2.025 |

**Appendix E. Linear thermal expansion of yttria**

| Temperature (°C) | Lattice parameter (A) | Percent linear expansion (%) |
|---|---|---|
| 25 | 10.6031 | 0.000 |
| 965 | 10.6770 | 0.696 |
| 1021 | 10.6855 | 0.777 |
| 1070 | 10.6949 | 0.865 |
| 1170 | 10.6982 | 0.896 |
| 1265 | 10.7080 | 0.989 |
| 1286 | 10.7119 | 1.026 |
| 1403 | 10.7220 | 1.121 |
| 1422 | 10.7255 | 1.154 |
| 1652 | 10.7550 | 1.432 |
| 1945 | 10.7900 | 1.762 |

## Appendix F. Linear thermal expansion of yttria-hafnia fluorite compositions

| Composition (mole % $Y_2O_3$) | Temperature (°C) | Lattice parameter (A) |
|---|---|---|
| 8 | 25 | 5.1204 |
| | 1028 | 5.1668 |
| | 1116 | 5.1698 |
| | 1167 | 5.1739 |
| | 1327 | 5.1845 |
| | 1453 | 5.1931 |
| | 1608 | 5.2046 |
| | 1756 | 5.2158 |
| | 1900 | 5.2262 |
| 14 | 25 | 5.1352 |
| | 927 | 5.1755 |
| | 1114 | 5.1849 |
| | 1280 | 5.1955 |
| | 1448 | 5.2101 |
| | 1467 | 5.2110 |
| | 1572 | 5.2184 |
| | 1607 | 5.2189 |
| | 1693 | 5.2218 |
| | 1755 | 5.2275 |
| | 1836 | 5.2379 |
| | 1894 | 5.2397 |
| 20 | 25 | 5.1502 |
| | 925 | 5.1930 |
| | 1140 | 5.2027 |
| | 1292 | 5.2132 |
| | 1436 | 5.2239 |
| | 1563 | 5.2328 |
| | 1677 | 5.2403 |
| | 1818 | 5.2526 |
| | 1898 | 5.2604 |
| 30 | 25 | 5.1842 |
| | 1058 | 5.2323 |
| | 1282 | 5.2481 |
| | 1477 | 5.2592 |
| | 1748 | 5.2775 |
| | 1897 | 5.2889 |

**Appendix F. (Continued)**

| Composition (mole % $Y_2O_3$) | Temperature (°C) | Lattice parameter (A) |
|---|---|---|
| 33.3 | 25 | 5.1965 |
| | 945 | 5.2410 |
| | 1086 | 5.2488 |
| | 1201 | 5.2555 |
| | 1207 | 5.2549 |
| | 1340 | 5.2645 |
| | 1386 | 5.2681 |
| | 1500 | 5.2745 |
| | 1516 | 5.2738 |
| | 1653 | 5.2803 |
| | 1727 | 5.2883 |
| | 1821 | 5.2931 |
| | 1913 | 5.3004 |
| 40 | 25 | 5.2154 |
| | 1030 | 5.2608 |
| | 1195 | 5.2738 |
| | 1400 | 5.2843 |
| | 1628 | 5.2981 |
| | 1921 | 5.3178 |
| 50 | 25 | 5.2364 |
| | 990 | 5.2822 |
| | 1127 | 5.2891 |
| | 1238 | 5.2949 |
| | 1362 | 5.3032 |
| | 1543 | 5.3118 |
| | 1779 | 5.3299 |
| | 1905 | 5.3406 |

**Appendix G. Axial and volume thermal expansion of monoclinic and tetragonal hafnia**

| Temperature (°C) | a (A) | b (A) | c (A) | $\beta$ (deg) | Unit cell volume ($A^3$) |
|---|---|---|---|---|---|
| 25 | 5.113* | 5.172 | 5.287 | 99.22 | 138.01 |
| 937 | 5.141 | 5.175 | 5.334 | 98.92 | 140.19 |
| 1052 | 5.148 | 5.178 | 5.341 | 98.96 | 140.63 |
| 1187 | 5.155 | 5.183 | 5.350 | 98.87 | 141.24 |
| 1232 | 5.164 | 5.186 | 5.360 | 98.77 | 141.87 |
| 1370 | 5.172 | 5.193 | 5.380 | 98.71 | 142.83 |
| 1482 | 5.175 | 5.185 | 5.388 | 98.54 | 142.97 |
| 1529 | 5.183 | 5.186 | 5.390 | 98.46 | 143.30 |
| 1580 | 5.178 | 5.185 | 5.390 | 98.36 | 143.17 |
| 1586 | 5.180 | 5.184 | 5.395 | 98.34 | 143.34 |
| 1590 | 5.173 | 5.182 | 5.393 | 98.36 | 143.03 |
| 1628 | 5.182 | 5.185 | 5.399 | 98.29 | 143.55 |
| 1652 | 5.186 | 5.182 | 5.406 | 98.18 | 143.80 |
| 1715 | 5.190 | 5.181 | 5.410 | 98.12 | 144.01 |
| 1763 | 5.150** | | 5.297 | | 140.49 |
| 1804 | 5.148 | | 5.295 | | 140.33 |
| 1825 | 5.154 | | 5.299 | | 140.76 |
| 1852 | 5.153 | | 5.302 | | 140.79 |
| 1862 | 5.152 | | 5.297 | | 140.60 |
| 1868 | 5.154 | | 5.300 | | 140.79 |
| 1913 | 5.158 | | 5.310 | | 141.27 |
| 1942 | 5.161 | | 5.307 | | 141.36 |

*The average standard deviation of the monoclinic parameters a, b, and c is 0.003 A and of $\beta$ is 0.03 deg. Standard deviations were determined by the computer program of Vogel and Kempter (40).

**The average standard deviation of each of the tetragonal parameters a and c is 0.002 A.

**Appendix H. Percent axial and volume thermal expansion of monoclinic and tetragonal hafnia**

| Temperature (°C) | Expansion of a (%) | Expansion of b (%) | Expansion of c (%) | Contraction of $\beta$ (%) | Volume Expansion (%) |
|---|---|---|---|---|---|
| 25 | 0.00 | 0.00 | 0.00 | 0.00 | 0.00 |
| 927 | 0.55 | 0.06 | 0.89 | 0.30 | 1.59 |
| 1052 | 0.69 | 0.12 | 1.02 | 0.26 | 1.90 |
| 1187 | 0.82 | 0.21 | 1.19 | 0.35 | 2.33 |
| 1232 | 1.00 | 0.27 | 1.38 | 0.45 | 2.80 |
| 1370 | 1.15 | 0.41 | 1.76 | 0.51 | 3.49 |
| 1482 | 1.21 | 0.25 | 1.91 | 0.69 | 3.60 |
| 1529 | 1.37 | 0.27 | 1.95 | 0.77 | 3.84 |
| 1580 | 1.27 | 0.25 | 1.95 | 0.87 | 3.74 |
| 1586 | 1.31 | 0.23 | 2.04 | 0.89 | 3.87 |
| 1590 | 1.17 | 0.19 | 2.01 | 0.87 | 3.64 |
| 1628 | 1.35 | 0.25 | 2.12 | 0.94 | 4.02 |
| 1652 | 1.43 | 0.19 | 2.25 | 1.05 | 4.20 |
| 1715 | 1.51 | 0.17 | 2.33 | 1.11 | 4.35 |
| 1763 | 0.72* | | 0.19 | | 1.80 |
| 1804 | 0.69 | | 0.15 | | 1.68 |
| 1825 | 0.80 | | 0.23 | | 2.00 |
| 1852 | 0.78 | | 0.28 | | 2.01 |
| 1862 | 0.76 | | 0.19 | | 1.88 |
| 1868 | 0.80 | | 0.25 | | 2.02 |
| 1913 | 0.88 | | 0.44 | | 2.37 |
| 1942 | 0.94 | | 0.38 | | 2.43 |

*Expansion of tetragonal parameters is based on the corresponding monoclinic parameters at 25°C.

## ACKNOWLEDGMENTS

The author wishes to thank his major professor, Dr. David R. Wilder, for his efforts in directing this research. A note of appreciation is extended to Dr. J. K. Johnstone and Dr. J. D. Schieltz for their helpful suggestions. The author expresses his sincere thanks to his wife, Karen, and his daughter, Kristi, for their encouragement during the course of this investigation and devoted effort in typing this dissertation.